Title

Structure-function analysis of *Arabidopsis* TOPLESS reveals conservation of repression mechanisms across eukaryotes

Authors

Alexander R. Leydon[1], Wei Wang[2,†], Samuel Juarez-Solis[1], Joseph E. Zemke[1], Mollye L. Zahler[1], Ning Zheng[2,3], Jennifer L. Nemhauser[1]

[1]Department of Biology, University of Washington
[2]Department of Pharmacology & [3]Howard Hughes Medical Institute, University of Washington
[†]Present address: Key Laboratory of Plant Stress Biology, State Key Laboratory of Cotton Biology, School of Life Science, Jinming Campus, Henan University, Kaifeng, Henan Province, 475004, PR of China.

Abstract

The corepressor TOPLESS (TPL) is recruited to many promoters, yet the mechanisms by which it inhibits expression of genes is poorly understood. Using a synthetic auxin response circuit in *Saccharomyces cerevisiae,* we identified two regions of *Arabidopsis thaliana* TPL that could independently function as repression domains: the LIS1 homology domain (LisH) and the CT11-RanBPM (CRA) domain. The CRA repressor domain required direct interaction with the Mediator subunit MED21 for full function. While corepressor multimerization is highly conserved, we found that multimer formation had minimal influence on TPL repression strength in yeast or in plants. Finally, we showed that the LisH domain may have a conserved role in repression in different proteins, as a LisH domain from the human TBL1 protein could replace TPL in synthetic assays. Our work provides insight into the molecular mechanisms of transcriptional repression, while also characterizing short, autonomous repression domains to augment synthetic biology toolkits.

Introduction

Control over gene expression is essential for life. This is especially evident during development when the switching of genes between active and repressed states drives fate determination. Mutations that interfere with repression lead to or exacerbate numerous cancers (Wong et al., 2014) and cause developmental defects in diverse organisms (Grbavec et al., 1998; Long et al., 2006), yet many questions remain about how cells induce, maintain, and relieve transcriptional repression. Transcriptional repression is controlled in part by a class of proteins known as corepressors that interact with DNA-binding transcription factors and actively recruit repressive machinery. Transcriptional corepressors are found in all eukaryotes and include the animal SMRT (silencing mediator of retinoic acid and thyroid hormone receptor) and NCoR (Nuclear receptor corepressor) complexes (Mottis et al., 2013; Oberoi et al., 2011), the yeast Tup1 (Matsumura et al., 2012), and its homologs Drosophila Groucho (Gro) and mammalian transducing-like enhancer (TLE) (Agarwal et al., 2015).

In plants, TOPLESS (TPL) and TOPLESS-RELATED (TPR1-4), LEUNIG (LUG) and its homolog (LUH), High Expression of Osmotically responsive genes 15 (HOS15) all act as Gro/TLE-type corepressors (Causier et al., 2012; Lee and Golz, 2012; Liu and Karmarkar, 2008; Long et al., 2006; Zhu et al., 2008). Defects in the TPL family have been linked to aberrant stem cell homeostasis (Busch et al., 2010), organ development (Gonzalez et al., 2015), and hormone signaling (Causier et al., 2012; Kagale et al., 2010), especially the plant hormone auxin (Long et al., 2006). Plant Gro/TLE-type corepressors share a general structure, where at the N-terminus a LIS1 homology (LisH) domain contributes to protein dimerization (Delto et al., 2015; Kim et al., 2004). At the C-terminus, WD40 repeats form beta-propeller structures involved in protein-protein interactions (Collins et al., 2019; Liu et al., 2019). In TPL family repressors, the LisH is followed by a C-terminal to LisH domain (CTLH) that binds transcriptional repressors through an Ethylene-responsive element binding factor-associated Amphiphilic Repression (EAR) motif (Causier et al., 2012; Kagale et al., 2010). The N-terminal domain also contains a CT11-RanBPM (CRA) domain, which provides a second TPL dimerization interface and stabilizes the LisH domain (Ke et al., 2015; Martin-Arevalillo et al., 2017). While the beta-propellers have been speculated to control protein interaction with other repressive machinery, they are known to bind the non-EAR TPL recruitment motifs found in transcriptional regulators (RLFGV- and DLN-type motifs, (Liu et al., 2019)).

We have previously demonstrated the recapitulation of the auxin response pathway by porting individual components of the *Arabidopsis* auxin nuclear response in yeast (Pierre-Jerome et al., 2014). In this Auxin Response Circuit (*At*ARC^{Sc}), an auxin responsive transcription factor called ARF binds to a promoter driving a fluorescent reporter. In the absence of auxin, the ARF protein activity is repressed by interaction with a full-length Aux/IAA protein fused to the N-terminal domain of TPL. Upon the

addition of auxin, the TPL-IAA fusion protein is targeted for degradation through interaction with a member of the Auxin Signaling F-box protein family (TIR1 or AFB2). Reporter activation can be quantified after auxin addition by microscopy and flow cytometry (Pierre-Jerome et al., 2014). In the original build and characterization of *At*ARC^{Sc}, it was noted that the two N-terminal truncations of TPL (N100 or N300) behave differently (Pierre-Jerome et al., 2014). While both truncations are able to repress the function of a transcriptional activator fused to an Aux/IAA, only the TPLN100 fusion shows alleviation of repression after auxin addition. TPLN300 fusions to Aux/IAAs maintain strong durable repression even in high concentrations of auxin. This disparity is not due to differential rates of protein degradation, as both proteins appear to be turned over with equal efficiency after auxin addition (Pierre-Jerome et al., 2014).

The crystal structure of the N-terminal domains of TPL homolog OsTPR2 from rice (Ke et al., 2015) and the *Arabidopsis* TPL (Martin-Arevalillo et al., 2017) have recently been solved. These structures reveal high conservation of protein folds in the N-terminus, as well as the residues that coordinate formation of homotetramers (Figure 1A). Several lines of evidence suggest that the multimeric TPL modulates repression potential. First, the first isolated and dominant TPL mutant *tpl-1* altered a single amino acid in the ninth helix of the TPL-N terminus (N176H) that induces aggregation of TPL and its homologs, reducing total activity (Long et al., 2006; Ma et al., 2017). Second, TPL recruitment motifs found in the rice strigolactone signaling repressor D53 induce higher order oligomerization of the TPL N-terminus, which increases histone binding and transcriptional repression (Ma et al., 2017). Third, structural studies of *Arabidopsis* TPL demonstrated interdependency of the TPL tetramer formation and Aux/IAA binding (Martin-Arevalillo et al., 2017). One contrary piece of evidence is the strong repressive activity of the TPL N100 construct which lacks the majority of the CRA domain ((Martin-Arevalillo et al., 2017), Figure 1A) and is therefore unlikely to be able to form tetramers.

The conservation of TPL's repressive function in yeast suggests that the protein partners that enact the repression are also likely to be conserved across eukaryotes. Consistent with this speculation, the series of alpha-helices that form the N-terminal portion of TPL is highly reminiscent of naturally occurring truncated forms of mammalian TLE (Gasperowicz and Otto, 2005), such as Amino-terminal Enhancer of Split (AES) (Zhang et al., 2010), the Groucho ortholog LSY-22 (Flowers et al., 2010), and the unrelated mouse repressor protein MXI1 (Schreiber-Agus et al., 1995). Gro/TLE family members are generally considered to repress by recruiting histone deacetylases to control chromatin compaction and availability for transcription (Chen and Courey, 2000; Long et al., 2006). An alternative hypothesis has been described for Tup1 in yeast, where Tup1 blocks the recruitment of Polymerase II (Pol-II) (Wong and Struhl, 2011), possibly through contacts with Mediator complex subunits MED21 or MED3 (Gromöller and Lehming, 2000; Papamichos-Chronakis et al., 2000). However, like many of these family members, multiple repression mechanisms have been described for TPL at

different genetic loci. For example, TPL has been found to recruit the repressive CDK8 Mediator complex (Ito et al., 2016), chromatin remodeling enzymes such as Histone Deacetylase 19 (HD19) (Long et al., 2006) and directly bind to histone proteins (Ma et al., 2017).

Here, we leveraged the power of yeast genetics to interrogate the mechanism of TPL repression. Using *At*ARC^{Sc}, we have discovered that the N-terminal domain of TPL contains two unique repression domains that can act independently. We have mapped the first repression domain to the first 18 amino acids of the LisH domain (Helix 1), and the second domain to Helix 8 which falls within the CRA domain. We have also identified critical residues required for repression in each domain. In addition, we found that that multimerization of TPL is not required for repression in yeast or in plants. We have also determined that full repression by Helix 8 requires direct interaction with MED21, and that this interaction requires the same MED21 residues that control transcriptional activation of Tup1-regulated genes in yeast. Finally, we found that LisH domains are a rich potential source of short, modular, sequence-diverse repression domains for complex synthetic circuits. An example is a single helix from the LisH domain of the human TBL1 protein, which was able to recapitulate TPL function.

Results

To understand how TPL represses transcription, we first sought to localize repressive activity within the protein. In the *At*ARC^{Sc}, the extent of auxin-induced turnover of TPLN100 and TPLN300 fusions appear similar, although neither are completely degraded (Pierre-Jerome et al., 2014). One interpretation is that auxin addition increases the sensitivity of the assay to detect subtle differences in the strength of repressive activity of each fusion protein by reducing its relative concentration—TPLN300 is a stronger repressor than TPLN100. To further exploit this synthetic repression assay, we began by generating a deletion series of the N-terminus guided by the available structural information (Ke et al., 2015; Martin-Arevalillo et al., 2017). We started with a TPLN188-IAA3 fusion protein construct, which behaves identically to TPLN300 (Pierre-Jerome et al., 2014), and subsequently deleted each alpha helical domain starting with Helix 9 (constructs are named in the format Helix x – Helix y or Hx-Hy). We found that Helix 8 was required for the maximum level of repression activity and for the maintenance of repression after auxin addition (Figure 1C). All constructs lacking Helix 8 retained the ability to repress transcription, but this repression was lifted in the presence of auxin (Figure 1C) as had been observed for the original TPLN100 construct (Pierre-Jerome et al., 2014). Further deletions revealed that including only the 18 amino acids of Helix 1 was sufficient to confer repression (H1, Figure 1D). To test whether Helix 8 activity depended on Helix 1, we tested an additional construct consisting solely of Helix 3 through Helix 9 (H3-H9, Figure 1D). This construct was also able to repress ARF activity, thus demonstrating that both Helix 1 (LisH) and Helix 8

(CRA) can act independently of one another (Figure 1D). To identify the minimal domain needed for Helix 8-based repression, we generated new deletions (Figure 1B,E-F). Helix 8 and the following linker were not sufficient for repression (Figure 1E), and removal of Helix 9 or of the linker between H8 and H9 slightly increased sensitivity to auxin (H1-H8Δ8L, Figure 1F). A deletion that removed both the LisH and Helix 8 repression domains (H3-H7) was only able to weakly repress reporter expression (Figure 1F). Together, these results demonstrate that Helix 1 and Helix 8 could act as repression domains, and that the linker between Helix 8 and Helix 9 (which folds over Helix 1) was required for repression following addition of auxin. Helix 1 alone in the LisH domain was sufficient to act on its own as a modular repression domain. The repressive activity of Helix 8 was only functional in the context of the larger Helix 3-Helix 8 truncation that carries the CTLH domain and a portion of the CRA domain.

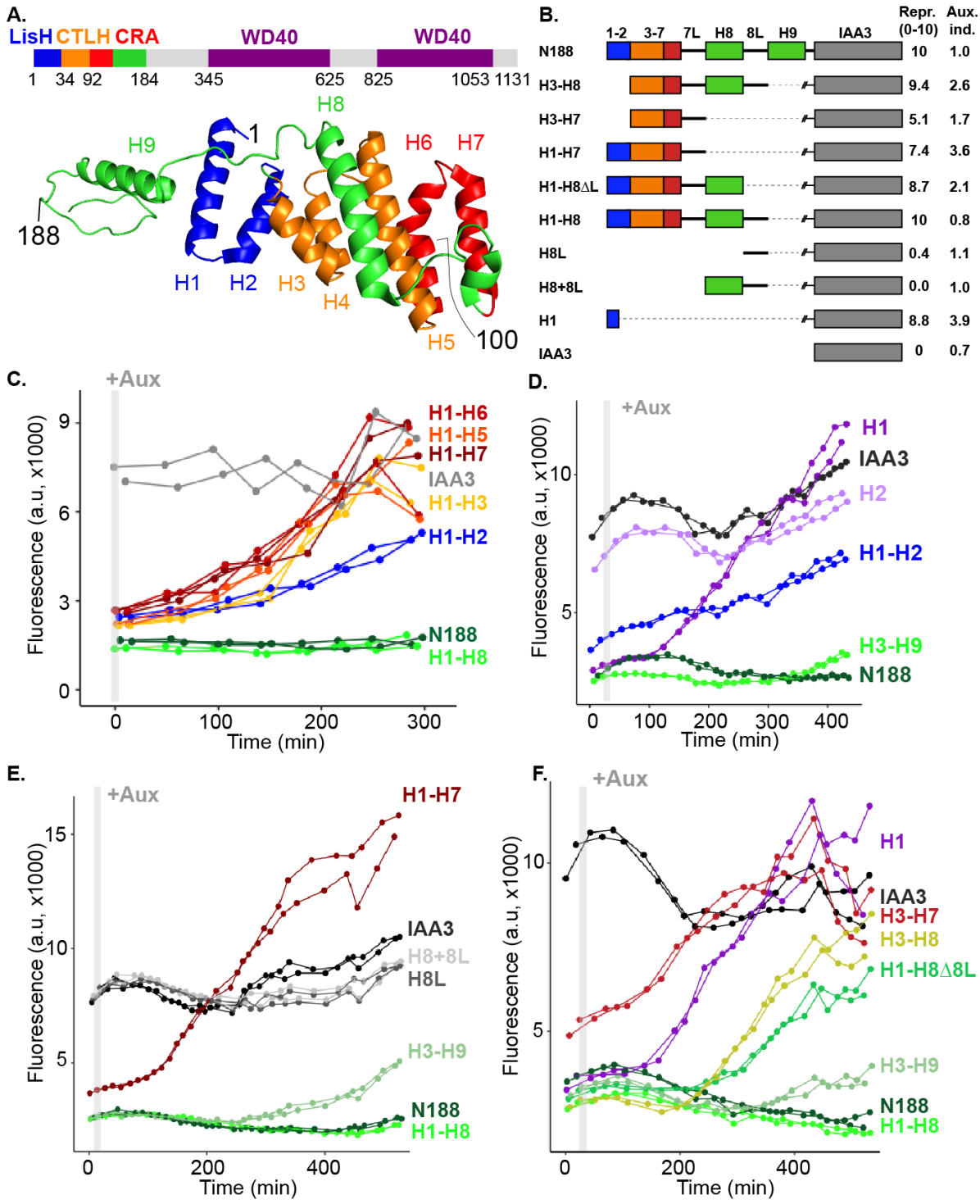

Figure 1. The N-terminal domain of TPL contains two independent repression domains. A. TPL domains are LisH (LIS1 homology motif, blue), CTLH (C-terminal LisH motif, orange), CRA (CT11-RanBPM, red - dimerization and green - foldback), and two WD40, beta-propeller motifs (purple). N-terminal domains are indicated on the solved structure of the first 202 amino acids ((Martin-Arevalillo et al., 2017), 5NQS). The termini of the TPL-N100 truncation used in the original ARC^{Sc} studies is indicated. **B.**

Diagram indicating the structure of constructs analyzed in experiments shown in subsequent panels. Repression Index (Rep.) is a scaled measure of repression strength with 0 set to the level of repression observed with IAA3 and 10 set to the level of repression by TPLN188-IAA3. Auxin induction level (Aux.) indicates the fold change difference between reporter expression before auxin addition (time zero) and at the end of an experiment (~500 minutes) **C-F.** Helix 1 and the CRA domain (Helix 3-Helix 8) can act independently to repress transcription. Each panel represents two independent time course flow cytometry experiments of the TPL helices indicated, all fused to IAA3. Every point represents the average fluorescence of 5-10,000 individually measured yeast cells (a.u. - arbitrary units). Auxin (IAA-10μM) was added at the indicated time (gray bar, + Aux).

To pinpoint which residues of Helix 1 and Helix 8 could coordinate repression through interaction with other transcriptional regulators, we identified likely solution-facing amino acids from each helix. We hypothesized that these amino acids were not involved in stabilizing the hydrophobic interactions between intra-TPL helical domains and could interact with partner proteins (Martin-Arevalillo et al., 2017). Six amino acids in Helix 1 and eight amino acids in Helix 8 were each mutated to alanine (Figure 2A,D, red residues) in the context of either H1-IAA3 or H3-H8-IAA3, respectively. Repression activity was assessed in the absence (Figure 2B,E) or presence (Figure 2C,F) of auxin. For Helix 1, the amino acids on either end of the helix (R6 and E18) were absolutely required for repression (Figure 2B). A mutation of E7, the immediate neighbor of R6, slightly increased reporter expression in the absence of auxin (Figure 2B) and lowered the final activation level after auxin addition when compared with wild type Helix 1 (Figure 2C). The R6A, E7A double mutation behaved similarly to the R6A single mutation. Likewise, the D17A, E18A double mutation did not enhance the effect of E18A alone. Q14 and D17 were indistinguishable from wild type Helix 1 (Figure 2C). In contrast to the other mutations which reduced Helix 1 repression activity or had no effect, F10A strengthened the durability of repression Helix 1, converting it into an auxin-insensitive Helix 8-type of repression domain (Figure 2C). In the context of the full-length N-terminus of TPL, F10 sits underneath the linker that connects Helix 8 to Helix 9, interacting with inward-facing hydrophobic cluster formed by F10 and F163, F33, F34 and L165 (Figure 2 – Figure Supplement 1A,B). It is likely that in any truncations where the linker is removed (i.e., H1-H2 through H1-H7 in Figure 1, and N100), F10 negatively affects repressor activity, possibly by decreasing binding affinity to putative interaction partners or the stability of protein complexes.

Unlike Helix 1, Helix 8 has an entirely solvent-exposed face, with eight amino acids that could be involved in protein-protein interactions. No single amino acid was essential for repression (Figure 2E). Two mutations (R140A and K148A) slightly increased baseline expression of the reporter (Figure 2D-F). All mutations, except

V145A and E152A that behaved as controls (data not shown), altered the stability of repression after auxin addition, either by increasing (S138A, E146A, K149A) or decreasing (I142A) the final fluorescence level (Figure 2F). Mutating E146 and K149 also increased the speed with which the reporter responded to auxin (Figure 2F), suggesting that these two neighboring residues could be a critical point of contact with co-repressive machinery. S138A had a small increase in auxin sensitivity, while I142 reduced auxin sensitivity (Figure 2F). TPL/TPR corerepressors are recruited to transcription factors through an Ethylene-responsive element binding factor-associated Amphiphilic Repression (EAR) motif (Causier et al., 2012; Kagale et al., 2010), which binds to the TPL in a pocket adjacent to Helix 8 (Ke et al., 2015; Martin-Arevalillo et al., 2017). While these two residues (S138A, I142) do not contact the conserved leucine residues of the EAR motif (LxLxL), in the AtTPL structure the C-terminal portion of the IAA27 EAR domain makes contact with these residues (Martin-Arevalillo et al., 2017). As we are using a TPL-IAA fusion protein, repression does not depend on EAR-TPL interaction, therefore making it difficult to fully assess any role this interaction normally plays in recruiting repression machinery (Figure 2 - Figure Supplement 1C).

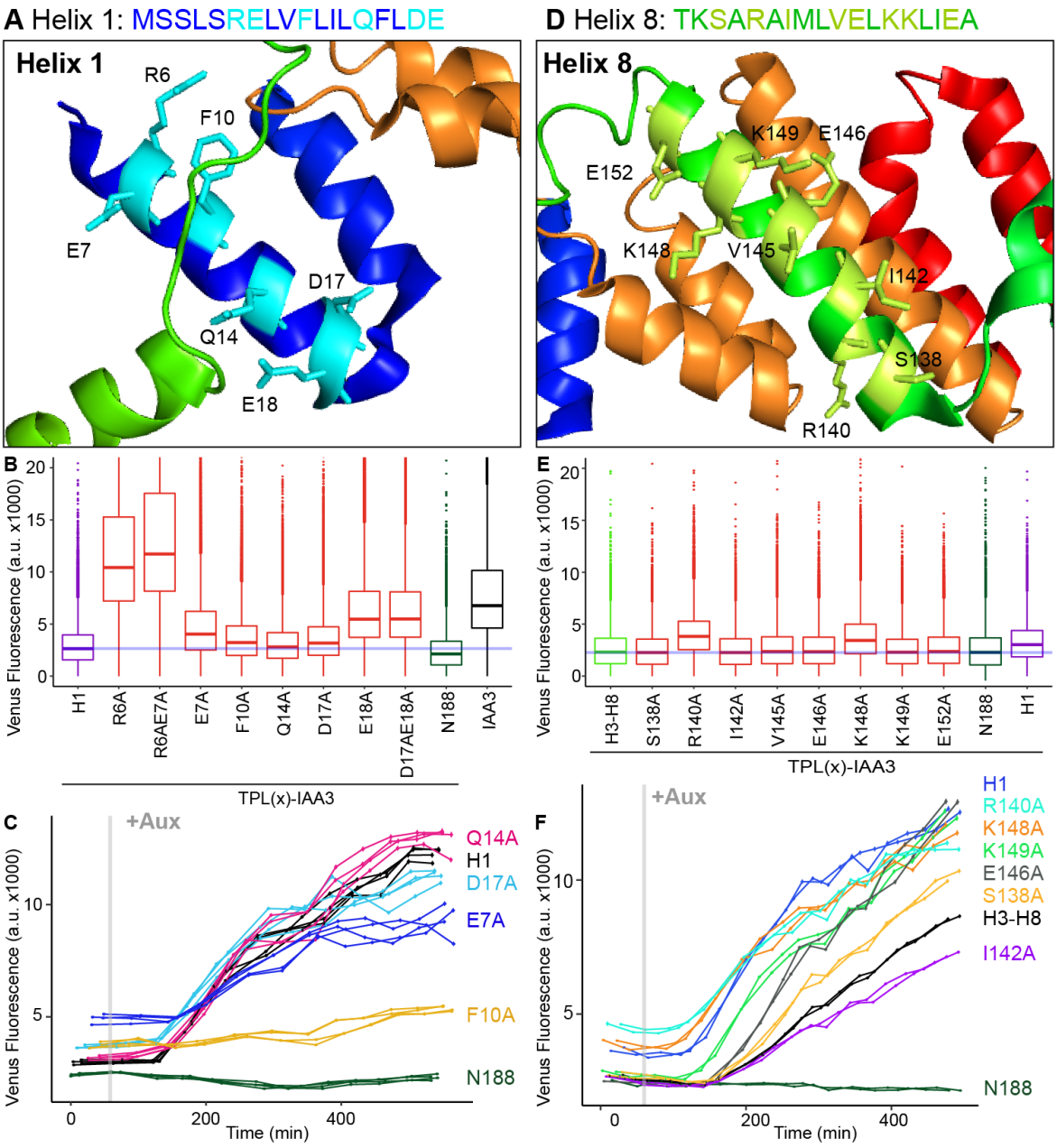

Figure 2. Identification of critical residues within each repression domain. A. Sequence and structure of Helix 1 (5NQS). The LisH domain is colored blue, and amino acids chosen for mutation are highlighted in both the sequence and the structure. **B.** Repression activity of indicated single and double alanine mutations. **C.** Time course flow cytometry of selected mutations of Helix 1 following auxin addition. **D.** Sequence and structure of Helix 8 (5NQS). Helix 8 is colored green, and amino acids chosen for mutation are highlighted in red in both the sequence and the structure. **E.** Repression activity of indicated alanine mutations. **F.** Time course flow cytometry of selected mutations of Helix 8 following auxin addition. For all cytometry experiments, the indicated TPL construct is fused to IAA3. Every point represents the average

fluorescence of 5-10,000 individually measured yeast cells (a.u. - arbitrary units). Auxin (IAA-10μM) was added at the indicated time (gray bar, + Aux). At least two independent experiments are shown for each construct.

To determine which of the many known or predicted TPL-binding partners could mediate the repression activity of Helix1 and Helix8, we identified known interactors with either TPL or other Gro/TLE co-repressors, and then introduced the *Arabidopsis* homologs of these genes into the cytoSUS system. Putative direct interactors include histone deacetylases (HDACs - AtHDAC9, AtHDAC6, (Long et al., 2006)), Histone proteins (Histone H3, Histone H4, (Ma et al., 2017)), and the Mediator components MED13 (AtMED13, (Ito et al., 2016)) and MED21, which has been demonstrated to interact with Tup1, the yeast homolog of TPL (Gromöller and Lehming, 2000). We did not observe any interactions between TPL-N188 and the HDACs HDA6 and HDA9; the histone protein AtHIS4; or the Mediator subunit AtMED13 (Figure 3A, Figure 3 – Figure Supplement 1A). HDAC interaction with TPL has been previously hypothesized to occur through indirect interactions with partner proteins (Krogan et al., 2012), however direct interactions with histones and MED13 have been detected (Ito et al., 2016; Ma et al., 2017). The absence of interaction between TPL-N188 and these proteins may be due to differences between methods, or interaction interfaces in the C-terminal WD40 repeats.

Strong interaction was detected between TPL-N188 and AtMED21 (Figure 3A). MED21 is one of the most highly conserved Mediator subunits (Bourbon, 2008), and has a particularly highly conserved N-terminus (Figure 3 – Figure Supplement 1A,C-E). In yeast, Tup1 interacts with the first 31 amino acids of ScMed21, with the first seven amino acids being absolutely required (Gromöller and Lehming, 2000). We observed that the equivalent truncation of AtMED21 (AtMED21-N31) was sufficient for interaction with TPL-N188 (Figure 3A). We next created truncations of the N-terminal domain of AtMED21 to closely match those that had been made in yeast (Figure 3B, Figure 3 – Figure Supplement 1B) where deletion of the first five amino acids of ScMed21 (ScΔ5Med21) severely reduce the ability of the Mediator complex to co-purify with Pol-II and CDK8 kinase complex (Sato et al., 2016). Interaction between TPLN188 and AtMED21 similarly required the first five amino acids of AtMED21 (Figure 3B), and this truncation did not significantly impact protein levels (Figure 3B).

We next tested which TPL repression domain interacted with AtMED21. We observed that AtMED21-N31 interacts with a construct containing Helix 8 (TPLH2-H9, Figure 3C), but not with a construct containing Helix 1 (TPLH1-H5, Figure 3 – Figure Supplement 3). We tested whether the residues in Helix 8 that were required for repression (V145, E146, K148, K149, Figure 2D-F) were also required for interaction with AtMED21. Single alanine mutations of these four amino acids in the context of TPLN188 significantly reduced interaction with AtMED21, while the quadruple mutation (here called Quad^{AAAA}) completely abrogated AtMED21 binding (Figure 3D). When

tested in the *At*ARC^{Sc}, TPLN188-Quad^{AAAA} resembled the repressive activity of wild-type N188 (red and black, Figure 3E), consistent with the observation that Helix 1 is sufficient for repression (Figure 1D). When F10 is buried under the linker between Helix 8 and Helix 9 (Figure 1 – Figure Supplement 1), or mutated to alanine (Figure 2C), Helix 1 is capable of driving auxin insensitive repression. Introduction of Quad^{AAAA} mutations into the Helix 3 through Helix 8 context (H3-H8-Quad^{AAAA}) largely phenocopied a Helix 3 through Helix 7 truncation (H3-H7, Figure 1F) with a drastically reduced repression strength and rapid alleviation of repression by auxin addition (yellow and pink, Figure 4E). These results indicate that the CRA domain (H3-H8) requires contact with MED21 to drive repression, and that this is independent of the repression through Helix 1.

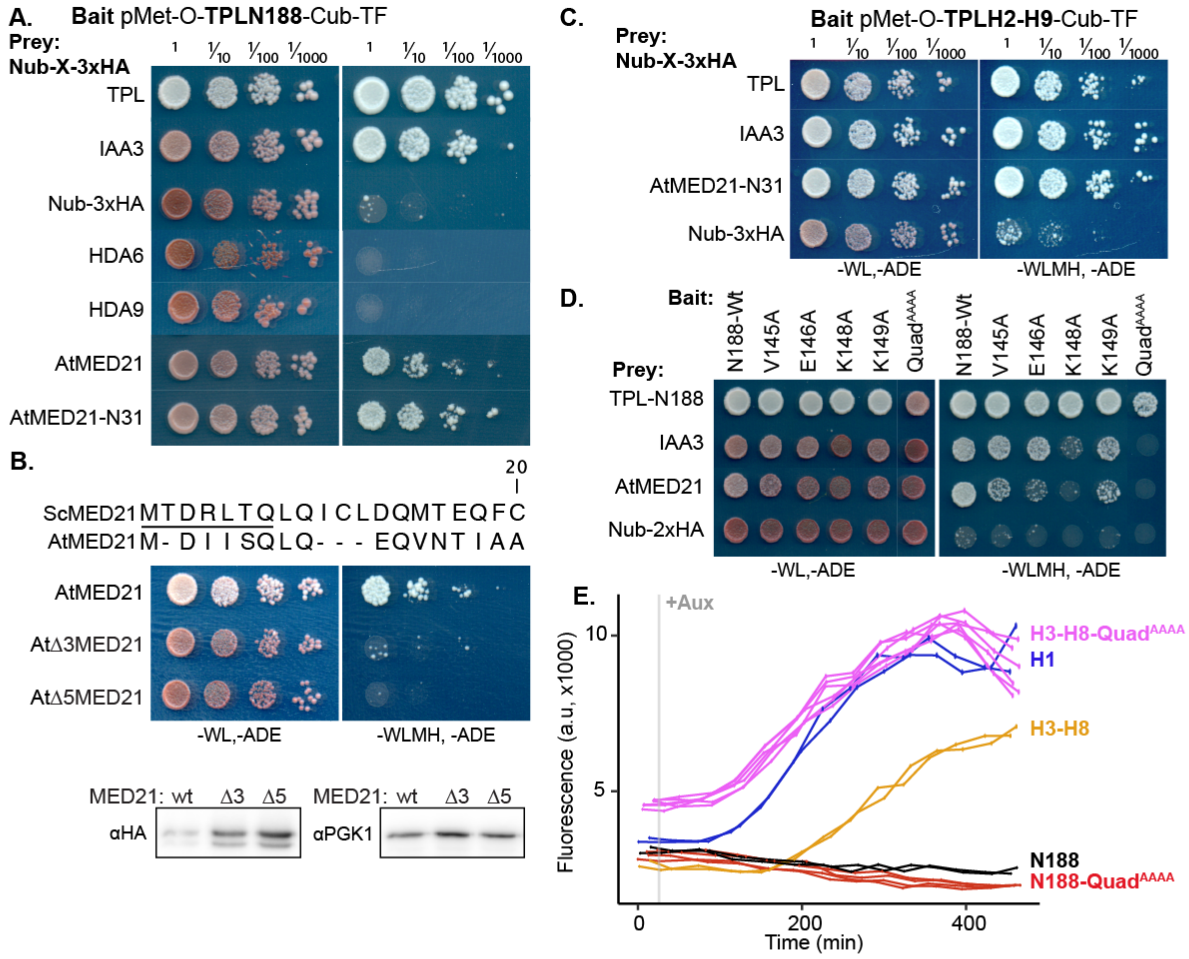

Figure 3. The Helix 8 repression domain of TPL directly interacts with MED21. A. cytoSUS assays with candidate interacting proteins. **B.** Alignments of the *Arabidopsis* (At) and *Saccharomyces* (Sc) MED21 proteins are shown above cytoSUS assays with the same bait shown in **A**. Western blots below the colonies indicated that AtMED21 N-terminal Δ3 and Δ5 are well expressed in assay conditions. **C.** A TPL-N truncation lacking Helix 1 (TPLH2-H9) could still interact with the AtMED21-N31 truncation. This

bait construct interacted with TPL-N188 and IAA3, but only minimally with the negative control (free Nub-3xHA). **D.** A series of alanine mutations (V145A, E146A, K148A, K149A, and the quadruple mutant Quad^{AAAA} chosen from Figure 2D-F) were introduced into the TPL-N188 bait construct and tested for interaction with wild-type TPL-N188, IAA3 and AtMED21. Each single alanine mutation reduces TPL interaction with AtMED21, while the quad mutation abrogated interaction. These mutations also reduced the binding strength of TPLN with IAA3, consistent with their position along the EAR binding pocket. **E.** The Helix 8 Quad^{AAAA} mutation was introduced into the TPLN188-IAA3 and TPLH3-8-IAA3 fusion proteins and compared to wild type N188 in time course flow cytometry. For all cytometry experiments, the indicated TPL construct is fused to IAA3. Every point represents the average fluorescence of 5-10,000 individually measured yeast cells (a.u. - arbitrary units). Auxin (IAA-10μM) was added at the indicated time (gray bar, + Aux). At least two independent experiments are shown for each construct.

To determine whether a protein-protein interaction is required for corepressor function, it is critical to demonstrate that reciprocal loss of function mutations activate repressed genes. In the case of Tup1, a standard approach has been to test deletion mutations of Tup1-interacting proteins to determine whether their interaction represents a true repression modality on the target gene (Gromöller and Lehming, 2000; Lee et al., 2000; Zhang and Reese, 2004). Deletion of the first 7 amino acids of ScMed21 (Δ7Med21) partially releases genes that are normally repressed by Tup1 into a transcriptionally active state (Gromöller and Lehming, 2000). We hypothesized that TPL repression would also be partially alleviated by such a deletion. Testing this hypothesis was complicated by the fact that ScMed21 is an essential gene, and yeast carrying deletions like Δ7Med21 grow more slowly (Gromöller and Lehming, 2000; Hallberg et al., 2006), which itself alters expression levels of reporters. In fact, even the Δ5Med21 yeast mutant has been demonstrated to alter Mediator assembly as the first 5 amino acids of ScMed21 are required for binding of Pol II and the CDK8 kinase module to the Mediator core (Hallberg et al., 2006; Sato et al., 2016). Therefore, we turned to the Anchor Away system for rapid, chemically conditional protein depletion (Haruki et al., 2008) to remove ScMed21 from the nucleus of yeast containing the auxin response circuit (Figure 4A). Anchor Away utilizes chemically dependent protein dimerization in the presence of Rapamycin to anchor target proteins in the cytoplasm, effectively removing their activity from the nucleus.

*At*ARC^{Sc} integrates components at four genomic locations using prototrophic markers that are not compatible with those needed for Anchor Away. To overcome this limitation, we re-recreated the entire ARC on a single plasmid (SLARC) using the Versatile Genetic Assembly System (VEGAS, (Mitchell et al., 2015)). SLARC behaved with similar dynamics to the original *At*ARC^{Sc} on both solid and liquid growth conditions

(Figure 4 – Figure Supplement 1). As a first test of the Anchor Away system with SLARC, we fused Tup1 and its partner protein Cyc8 to two copies of the FKBP12-rapamycin-binding (FRB) domain of human mTOR (Haruki et al., 2008). Rapamycin treatment of strains targeting either of these proteins caused no release of repression, providing confirmation that the ARC acts orthogonally to the yeast corepressor (Figure 4 – Figure Supplement 2).

We introduced SLARCs with different TPL constructs into strains where ScMed21 wild-type or N-terminal deletions were targets of Anchor Away. Strains expressing ScMed21 with or without FRB fusions behaved similarly (Figure 4B, Figure 4 – Figure Supplement 3). We then compared the transcriptional output of the fully repressed SLARC^{N188} in MED21 N-terminal mutants lacking the first 3, 5 or 7 amino acids. We observed that all three deletions significantly increased the expression of the reporter in SLARC^{N188}, while no mutation increased the SLARC's sensitivity to auxin (Figure 4B, Figure 4 – Figure Supplement 3) as expected from the TPL truncation data (Figure 3E). As Δ7ScMed21 did not increase reporter expression when compared to Δ5ScMed21 yet did have a noticeable impact on growth, we eliminated it from further analyses. Deletions of ScMed21 N-terminal residues impairs auxin responsive transcriptional activation in SLARC$^{H1\text{-}H5}$ (Figure 4C), consistent with the role of this region in promoting Pol-II recruitment (Sato et al., 2016). The fully repressed SLARC^{N188} demonstrated no auxin sensitivity in Δ3ScMed21 or Δ5ScMed21 mutants, yet showed elevated transcription of the reporter (Figure 4D). Conversion of the first five amino acids of ScMed21 to the corresponding sequence from AtMED21 resulted in an identical repression profile (Figure 4 – Figure Supplement 4A), and had no effect on yeast growth or viability (Figure 4 – Figure Supplement 4B), further highlighting the conservation of this repression mechanism between the two organisms.

The stably expressed N-terminal deletions of ScMed21 likely alter the expression of multiple yeast genes, and this state change could confound our interpretations of the importance of ScMed21 on TPL repression. To minimize the off-target impact of ScMed21 deletions, we introduced estradiol inducible versions of ScMed21 (iScMed21) into the Anchor Away SLARC^{N188} strains (Figure 4A, (McIsaac et al., 2013)). The combination of all three synthetic systems made it possible to rapidly deplete the wild type ScMed21-FRB from the nucleus while simultaneously inducing ScMed21 variants and visualizing the impact on a single auxin-regulated locus. Depletion of nuclear ScMED21 by Rapamycin increased levels of the reporter in all genotypes examined (Figure 4D) while also increasing cell size even in short time-courses, consistent with its essential role in many core pathways (Figure 4 – Figure Supplement 5A, (Gromöller and Lehming, 2000)). When wild-type iScMed21 was induced, there was a rescue of both phenotypes (Figure 5E, black), whereas induction of either Δ3 and Δ5 variants recapitulated the reporter activation seen in the stably expressed mutant versions (Figure 4E, green and blue, Figure 4 – Figure Supplement 5B). iΔ3Med21 was induced

and accumulated at a comparable level to wild type MED21, while Δ5 appears to be less stable (Figure 4F). In these short time courses, we did not observe the cell size increases observed in the Rapamycin treatments (populations were evenly distributed around a single mean, suggesting we were observing the immediate effects of the MED21 deletions (Figure 4 – Figure Supplement 5C-D)).

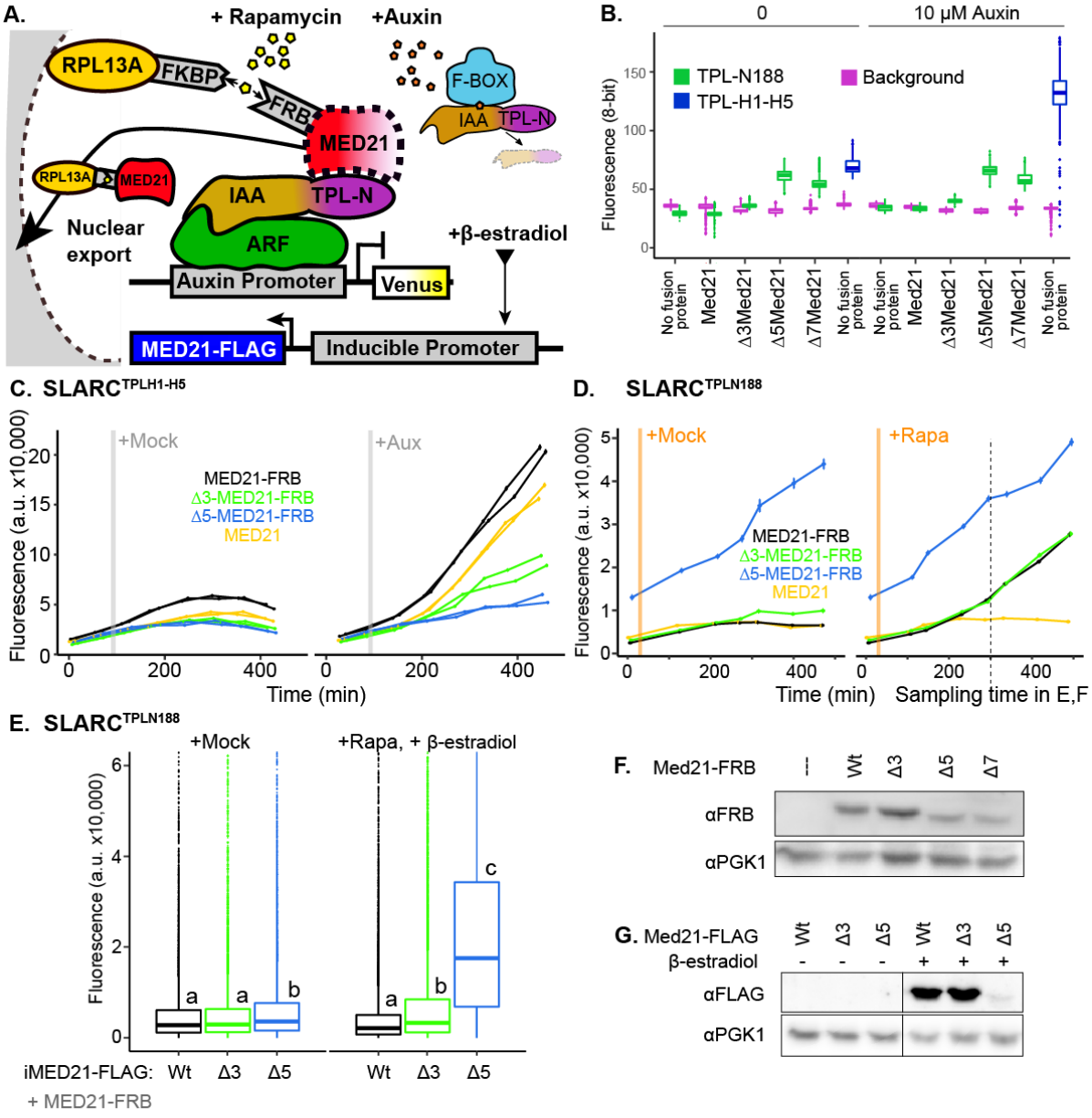

Figure 4. Repression by TPL requires interaction with the N-terminus of MED21.
A. Schematic of *At*ARC^{Sc} combined with methods for inducible expression and nuclear depletion of MED21. In Anchor Away, the yeast ribosomal protein 13A (RPL13A) is fused to the rapamycin binding protein FKBP. Addition of Rapamycin induces dimerization between FKBP and any target protein fused to FRB, resulting in removal of

the target protein from the nucleus. For these experiments, *At*ARC^{Sc} was assembled into a single plasmid (SLARC) rather than being integrated into separate genomic loci (Figure 4 – Figure Supplement 1). Estradiol-inducible ScMed21 (iMed21) made it possible to replace wild-type MED21 with targeted deletions or mutations. **B.** Quantification of Venus fluorescence from SLARC^{N188} in wild type and N-terminal ScMed21 deletions with and without auxin. Yeast was grown for 48 hours on SDO media with or without auxin and colony fluorescence was quantified and plotted with the auxin responsive SLARC^{H1-H5} in wild type as a reference. Red autofluorescence was used as a reference for total cell density. **C.** Time-course flow cytometry analysis of SLARC^{H1-H5} in wild type and n-terminal ScMed21 deletions with and without auxin. Genotypes are indicated in the colored key inset into the graph. Auxin (IAA-10μM) was added at the indicated time (gray bar, + Aux). **D.** Time-course flow cytometry analysis of SLARC^{N188} in wild type and N-terminal ScMed21 deletions with and without Rapamycin. Genotypes are indicated in the colored key inset into the graph. For (**C-D**) a.u. - arbitrary units. Rapamycin was added at the indicated time (orange bar, + Rapa). Every point represents the average fluorescence of 5-10,000 individually measured yeast cells. **E.** Rapid replacement of Med21-FRB with inducible Med21-FLAG demonstrated the requirement for the ScMed21 N-terminus in TPL repression. iMed21 isoforms were induced by addition of β-estradiol (20μM) for 4 hours followed by Rapamycin addition. Fluorescence was quantified by cytometry after 300 minutes (indicated by dashed box in **D**). Lower case letters indicate significant difference (ANOVA and Tukey HSD multiple comparison test; $p<0.001$). **F-G.** Protein abundance of ScMed21 variants was tested by SDS-PAGE & western blot.

Another potential mechanism for TPL repression is multimerization, as both the N-terminus of AtTPL and OsTPR2 adopt a tetrameric form when crystallized (Figure 5A (Ke et al., 2015; Martin-Arevalillo et al., 2017)). We used the cytoplasmic split ubiquitin (cytoSUS) protein-protein interaction assay (Asseck and Grefen, 2018) to begin to test this hypothesis. We observed that Helix 8 was required for strongest interaction between TPL constructs (Figure 5 – Figure Supplement 1A), although this assessment was complicated by the fact that some of the shorter constructs accumulated to significantly lower levels (Figure 5 – Figure Supplement 1B). The weak interaction we could observe between full length TPL-N and the Helix 1 through Helix 3 construct (H1-3), indicated that the TPL LisH domain is sufficient for dimerization. Therefore, while auxin-insensitive repression may require multimeric TPL, this higher order complex was not required for auxin-sensitive repression mediated by Helix 1 (Figure 1C-D). In their study of the AtTPL structure, Martin-Arevalillo et al. identified a triple mutation (K102S-T116A-Q117S-E122S) that abrogated the ability of the CRA domain (Helix 6 and Helix 7) to form inter-TPL interactions (Martin-Arevalillo et al., 2017). As this mutant form of TPL is only capable of dimerizing through its LisH domain, we refer to it here as LDimer

(Figure 5A). The LDimer mutations in TPLN188 retained the same auxin insensitive repression auxin behavior as wild-type TPLN188 (Figure 5D), supporting the finding from the deletion series.

To make a fully monomeric form of TPL, we introduced mutations into the dimerization interface of the LisH domain in the context of LDimer. We first mutated one of a pair of interacting residues (F15) to a series of amino acids (Tyrosine - Y, Alanine - A, Arginine - R, or Aspartic Acid - D) in the context of either LDimer (Figure 5D), or H1-2 (Figure 5B, 5E). We observed that conversion of F15 to the polar and charged aspartic acid (D) completely abolished repression activity, while the polar and positively charged arginine was better tolerated (Figure 5D,E). The conversion of F15 to tyrosine had no effect on LDimer (Figure 5D), and only a minimal increase in auxin sensitivity in the context of H1-2 (Figure 5E). We then combined LDimer-F15Y with a mutation of the coordinating residue L8 to serine with the intention of stabilizing the now solvent-facing residues. The repressive behavior of this mutant was indistinguishable from that of LDimer (Figure 5F). To further push the LDimer towards a monomeric form, we introduced two additional mutations (S5A, E19S, Figure 5C,G). Size exclusion chromatography confirmed that this combination of mutations (S5A-L8S-F15Y-E19S-K102S-T116A-Q117S-E122S, hereafter called Monomer) successfully shifted the majority of the protein into a monomeric state (Figure 5H); however, this shift had no observable impact on repression strength before or after auxin addition (Figure 5G). To test whether these mutations had a similar impact on *in vivo* TPL complexes, we introduced the LDimer and Monomer mutations into the cytoSUS assay. In contrast to the *in vitro* chromatography results with purified proteins, Monomer expressed in yeast retained measurable interaction with wild-type TPL, LDimer or Monomer, albeit at a reduced level than what was observed between two wild type TPLN188 constructs (Figure 5I). A caveat to this apparent difference between assays is that the Monomer mutations led to a striking increase in protein concentration in yeast (Figure 5 – Figure Supplement 1C), likely partially compensating for the decrease in affinity.

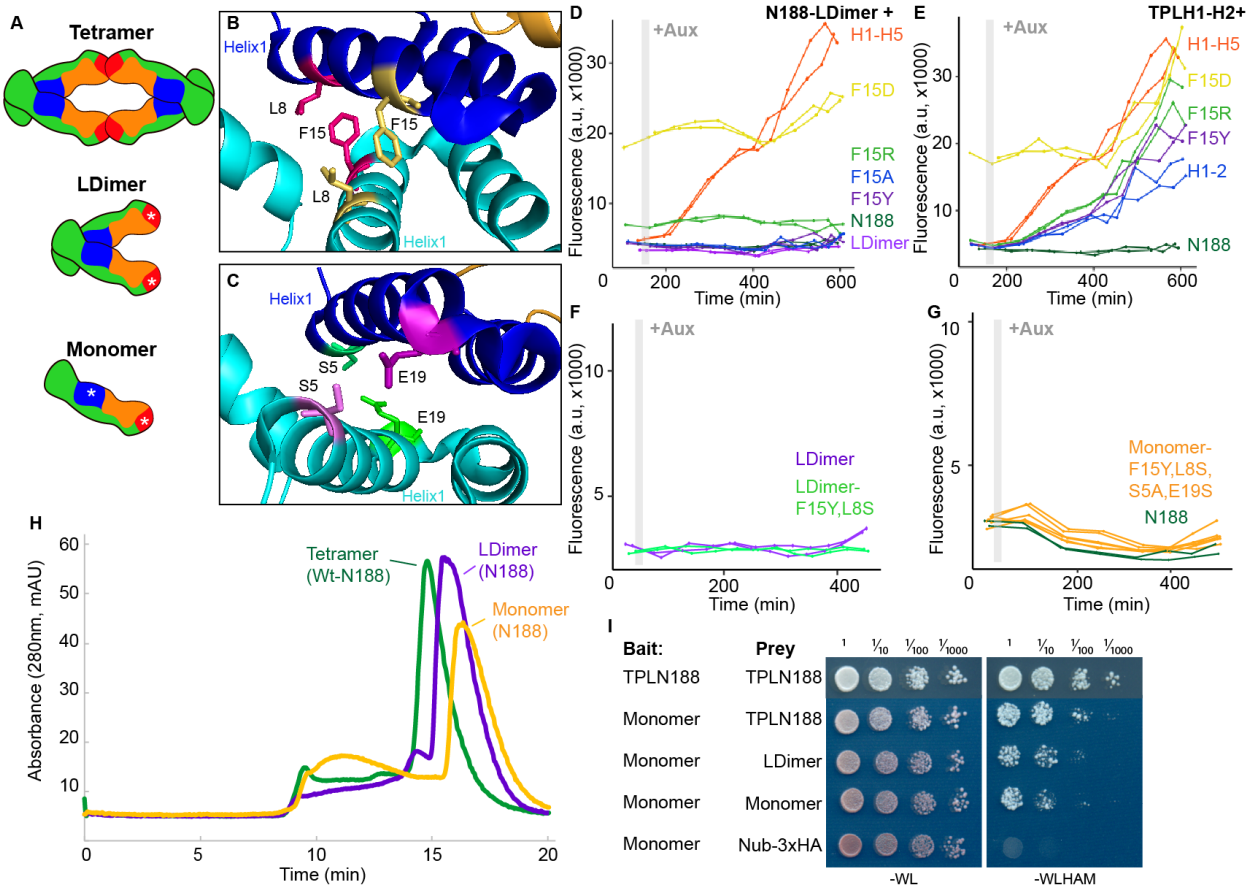

Figure 5. Multimerization is not required for repression in yeast. A. TPL can form a homotetramer via the CRA (red) and LisH (blue) domains. Asterisks indicate mutations that block or diminish these interactions. **B-C**. Locations of critical positions in Helix 1 are highlighted for two interacting TPL monomers (shown in light and dark blue). Interacting amino acids share the same color (adapted from 5NQV). **D-G.** Time course flow cytometry analysis of TPLN-IAA3 fusion proteins carrying selected single point mutations in N188-LDimer-IAA3 (**D**) and the TPLH1-2 truncation (**E**). The F15Y mutation had little effect on repression activity for either TPL construct. Double mutations (F15Y, L8S in LDimer) (**F**) or the quadruple Monomer mutations (S5A, L8S, F15Y, E19S in LDimer) (**G**) showed repression activity that was indistinguishable from LDimer or wild type N188 fused to IAA3. For all cytometry experiments, the indicated TPL construct is fused to IAA3. Every point represents the average fluorescence of 5-10,000 individually measured yeast cells (a.u. - arbitrary units). Auxin (IAA-10μM) was added at the indicated time (gray bar, + Aux). At least two independent experiments are shown for each construct. **H**. Size Exclusion Chromatography on TPLN188 wild type (green), LDimer (purple) and Monomer (orange) tetramerization mutants. **I**. CytoSUS on TPL tetramerization mutants.

While the *At*ARC^{Sc} relies on the strong conservation of the core regulatory machinery in yeast and plants, there are important differences between the synthetic and native systems. For example, while the TPL-N188 construct (and other variants that contain Helix 8 and the linker between Helix 8 and Helix 9) repressed transcription in yeast even after auxin addition, this is not the case for the many auxin-regulated genes in plants. To probe these differences, we created a conditional expression system for plants that was based on the UAS/GAL4-VP16 system (Brand and Perrimon, 1993). In this system, the synthetic transcription factor GAL4-VP16 drove expression of a TPLN-IAA14 fusion protein that could dominantly repress the auxin response (Figure 6A). We engineered a variant of *IAA14* called *IAA14^{mED}* which carries mutations in the EAR domain (EAR^{AAA}) and in the degron (P306S) to block interference from the endogenous TPL/TPRs and TIR1/AFBs, respectively (Figure 6A). After prototyping the system in yeast (Figure 6- Figure Supplement 1), we transiently transformed constructs carrying *TPLN-IAA14^{mED}* variants into *Nicotiana benthamiana* (tobacco) to test levels of repression of the well-characterized auxin response promoter DR5 (Ulmasov et al., 1997). Co-infection with *AtARF19* resulted in a roughly 3-fold increase in reporter activity (Figure 6B), sensitizing the system to detect variations in repression activity. *UAS-TPLN188-IAA14^{mED}* was able to repress reporter expression in tobacco leaves when co-expressed with *GAL4-VP16* and *AtARF19* (Figure 6B). We observed strong correlation in repression activity between *At*ARC^{Sc} and the transient overexpression system in tobacco for most TPL variants. Truncations containing Helix 1 (H1, H1-2, H1-5) or helix 8 (H3-8), as well as the full N-terminus (N188) repressed the DR5 reporter (Figure 6B). LDimer and Monomer variants retained a similarly strong repressive activity in tobacco as what had been observed in yeast (Figure 6B). There were some differences between the systems. Constructs with Helix 1 alone were less efficient repressors in tobacco, and the F10A mutation had little to no impact on repression strength (H1-F10A, N188-F10A, Figure 6B).

We were concerned that the lack of effect of multimerization mutants (LDimer and Monomer) on repression strength could still be a product of heterologous expression. To test the effect of these mutants in a native context, we generated transgenic *Arabidopsis* lines where the UAS-TPL-IAA14^{mED} constructs were activated in the root pericycle cells where IAA14 normally functions to regulate initiation of new roots (Figure 6C, inset). To do this, we first had to introgress the J0121 enhancer trap which drives expression of both GAL4-VP16 and GFP in pericycle cells (Laplaze et al., 2005) into Col-0 (J0121^{Col-0}). We then transformed J0121^{Col-0} with our UAS-TPL-IAA14^{mED} constructs. A plant carrying a functional TPL variant fused to a stabilized IAA14 should make very few if any lateral roots, phenocopying the original solitary root (*slr*) mutant (Fukaki et al., 2002). As expected, transformants expressing either IAA14^{mED} (with no TPL fusion) or TPLN188 (with no IAA14 fusion) had no effect on lateral root production. In contrast, TPLN188-IAA14^{mED} fusion constructs sharply decreased lateral root density

(Figure 6C). Both LDimer-IAA14^{mED} and Monomer-IAA14^{mED} constructs (Figure 6C) were able to repress lateral root development, suggesting that multimer formation is not required for TPL repression of native auxin-induced genes.

In addition to understanding the native function of TPL, we were also interested in characterizing minimal, orthogonal repression domains to use in synthetic circuits. At 18 amino acids long, TPL-H1 is among the shortest repression domains identified to date, and it functions in both yeast and plants (Figures 1D, 2A-D, 6B). Residues within Helix 1 are highly conserved within *Arabidopsis* accessions (Hamm et al., 2019), and this conservation can be observed as far back as Embryophytes (approximately 400 million years of conservation (Martin-Arevalillo et al., 2019), Figure 6 – Figure supplement 2). LisH domains are found in diverse proteins across eukaryotes, and we were curious whether other LisH -containing proteins could be mined for similar short, modular repression domains. A phylogenic tree revealed a cluster of LisH-containing proteins characterized as having repressor activity (Figure 6 – Figure Supplement 3). This cluster included TBL1 from humans (Oberoi et al., 2011) and HOS15 from *Arabidopsis* (Mayer et al., 2019). An alignment of selected LisH domains within this clade (PF08513) revealed extensive sequence diversity, especially within the regions homologous to Helix 1 (Figure 6D, Figure 6 – Figure Supplement 3). As there is a striking similarity in TPL and TBL1 structures (Martin-Arevalillo et al., 2017), we used TBL1 as a proof-of-principle for identifying new modular repression domains. We found that indeed the first 98 amino acids of TBL1 fused to IAA3 could act as a repression domain (Figure 6F), and a truncation containing only the first helix of the LisH domain (TBL1-H1) had an equally high level of repressive activity. Like TPL-H1, repression by TBL-H1 was also reversed by addition of auxin (Figure 6E). TBL1N98 doesn't interact with ScMed21 or AtMED21 (Figure 6 – Figure Supplement 4), consistent with this interaction residing in Helix 8 of TPL.

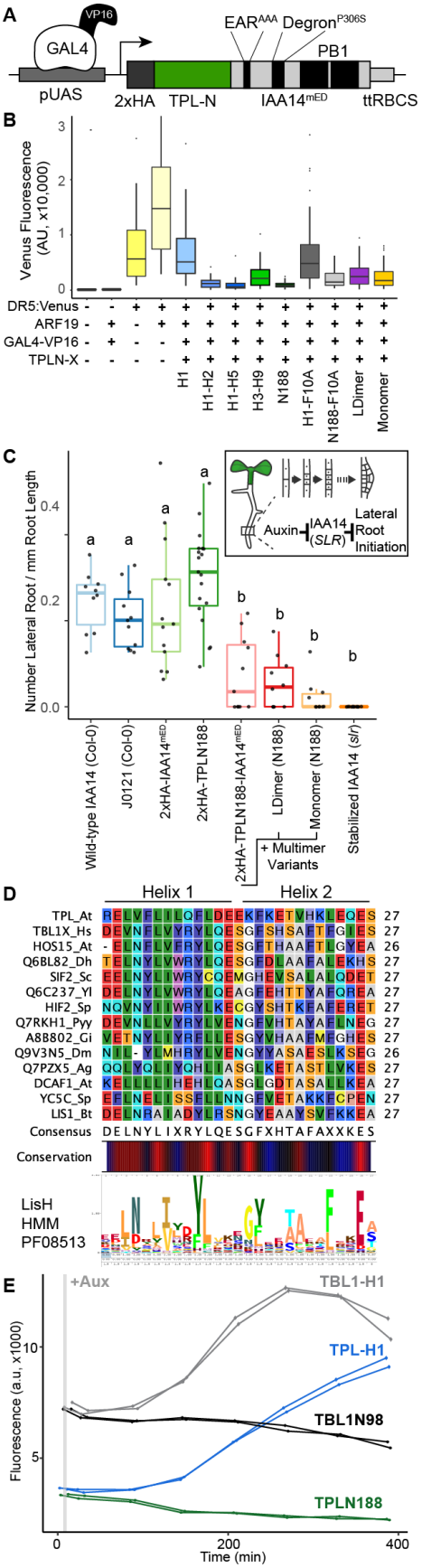

Figure 6. TPL repression domains behave similarly in yeast and plants, and they can be used to identify novel repression domains from structurally-related proteins. A. Design of UAS-TPL-IAA14^{mED} constructs. Mutation of the conserved Lysine residues in the EAR domain disrupted potential interactions with endogenous TPL/TPR proteins. The IAA14 degron has been mutated (P306S) to render it auxin insensitive. UAS – upstream activating sequence, ttRBCS - Rubisco terminator sequence. **B.** Transient expression of indicated TPL constructs in *Nicotiana benthamiana* leaves. DR5:Venus - the synthetic DR5 auxin promoter (Ulmasov et al., 1997) driving Venus, ARF19 - p35S:AtARF19-1xFLAG, GAL4:VP16 - pUBQ10:GAL4-VP16, TPLN-X - UAS-TPL-IAA14^{mED} with various TPL truncations or mutations. **C.** Auxin induced degradation of IAA14 is absolutely required for initiation of lateral root development (cartoon inset). N-terminal domains of TPL were sufficient to repress the development of lateral roots in *Arabidopsis* seedlings. The density of emerged lateral roots was measured in T1 seedlings at 14 days after germination. Lower case letters indicate significant difference (ANOVA and Tukey HSD multiple comparison test; $p<0.001$). **D.** Alignment of TPL with related LisH domains from PFAM08513. Residues are colored according to the Rasmol color scheme. The LisH Hidden Markov Models (HMM) from PFAM is aligned below to allow interpretation of broader LisH domain conservation (Schuster-Böckler et al., 2004). **E.** The Human TBL1 N-terminal domain could replace TPL in *At*ARC^{Sc}. The TBL1 N terminus (N98) or the TBL1 Helix 1 (TBL1-H1) was translationally fused to IAA3 and compared to TPLN188 and TPLH1 in time course auxin response assays. Auxin (IAA-10μM) was added at the indicated time (gray bar, + Aux).

Discussion

A review of the current literature on corepressors gives the conflicting impressions that (a) corepressor function is broadly conserved, and (b) that every organism (and perhaps even each corepressor) has a distinct mode for transcriptional repression (Adams et al., 2018; Mottis et al., 2013; Perissi et al., 2010; Wong and Struhl, 2011). We hoped that the *At*ARC^{Sc} could facilitate a resolution to this apparent contradiction by targeting repression to a single synthetic locus. We focused our initial efforts on the analysis of the N-terminal portion of TPL which has multiple known protein-protein interaction surfaces (Ke et al., 2015; Martin-Arevalillo et al., 2017). Experiments with the *At*ARC^{Sc} identified two repression domains [Helix 1 and Helix 8 (Figures 1-2)] within the N-terminus of TPL, both of which were subsequently confirmed to repress transcription in plants as well. Amino acids within each helix that were critical for repression activity have their R-groups oriented away from the hydrophobic core of TPL structure. This led us to hypothesize that they are therefore likely contact points for other proteins (Figure 2). In the case of Helix 8, we were able to identify one of these partners—MED21—a Mediator subunit that also interacts with the yeast corepressor Tup1 (Figure 3, 4). This result suggests a fundamental conservation in at least one corepressor mechanism across species. Contrary to our initial hypothesis, the monomeric form of TPL was sufficient for strong repression in yeast and in plants, leaving open the question of the role of higher-order TPL complex formation (Figure 5). Finally, we were able to show that the Helix 1 repression domain can be used to identify additional modular repression domains from diverse species (Figure 6).

The Mediator complex is a multi-subunit complex that connects DNA-bound transcription factors and the RNA polymerase II complex (Pol-II) to coordinate gene expression, first identified in yeast (Flanagan et al., 1991; Kim et al., 1994). The Mediator subunits in yeast are organized into four separate modules; head, middle, tail and kinase, with a strong conservation of module components in plants (Dolan and Chapple, 2017; Maji et al., 2019; Malik et al., 2017; Samanta and Thakur, 2015). MED21 forms a heterodimer with MED7 to create the central region of the Middle region of the Mediator complex, and the MED21 N-terminus is centered on a flexible hinge region (Baumli et al., 2005), which is required for Pol-II recruitment and CDK8 kinase module recruitment (Sato et al., 2016). The protein interaction between TPL and MED21 occurs at the N-terminus of MED21, highlighting the importance of this region as a signaling hub (Sato et al., 2016). Other lines of evidence support this role, as this region binds the yeast homolog of TPL, Tup1 (Gromöller and Lehming, 2000) through a completely different protein domain as no homology can be found between TPL helix 8 and Tup1 in any region by primary amino acid homology (i.e. BLAST).

Corepressors coordinate multiple mechanisms of repression through discrete protein interactions, leading to robust control over eukaryotic transcription by combining repression modalities. Corepressor function has variously been linked to (i) altering

chromatin confirmation, often through interaction with histone modifying proteins or histone proteins themselves, (ii) direct interference with transcription factor binding or function and (iii) physical spreading of long-range oligomeric corepressor complexes across regions of regulatory DNA (Perissi et al., 2010). Dissection of the importance of each modality in Tup1 repression has been challenging (Lee et al., 2000; Zhang and Reese, 2004). The tour-de-force of corepressor mechanism studies in yeast concluded that the primary function of Tup1 was to physically block activators (Wong and Struhl, 2011). In this work, the authors utilized the Anchor Away approach to correlate the importance of HDACs, transcriptional machinery and chromatin remodeling enzymes to the repression state of endogenously repressed Cyc8-Tup1 target genes. They observed that Tup1 did not block the binding of transcription factors but inhibited the recruitment of one Mediator component in the tail domain, GAL11/MED15, as well as Pol-II and the chromatin remodelers Snf2 and Sth1. They additionally observed that HDACs had only a supportive role in reinforcing Tup1 repression. These results led to their hypothesis that Tup1 blocks the activation domains of transcription factors, and suggested this was through direct binding to activation domains (Wong and Struhl, 2011).

The synthetic system used here allowed us to build on this model and further refine our understanding of TPL's repressive activity. In our experiments we see a similar set of conditions, with TPL recruited to the DNA-bound transcriptional activator (ARF), and several possible mechanisms of repression. Unlike Tup1, we have subdivided the TPL protein to identify interactions between TPL and individual protein interactors with no effect on yeast function. In these experiments we can eliminate the possibility that TPL blocks ARF activation by directly blocking the transcription factor activation domains because we see a loss of repression only when TPL-MED21 binding is eliminated through specific point mutations (Figure 3E). Our inducible swap of MED21 isoforms also corroborates these findings (Figure 4), as the SLARC remains genetically identical in these strains, indicating that TPL-MED21 interaction is regulating activity not a TPL-ARF interaction. Furthermore, our results correlate well with findings that repressed targets are reactivated when this portion of MED21 is deleted in yeast (TPL - Figure 4, Tup1 - (Gromöller and Lehming, 2000)). Therefore, we suggest that instead of directly binding activation domains that TPL (and likely Tup1) binds to components of Mediator (MED21 and possibly others) recruited by the transcription factor. Indeed, it is easier to rationalize that the repressor binds the same domains of the Mediator complex recruited by the transcription factor's activation domain (with the same affinity) as opposed to binding each diverse activation domain (with varying affinity). In this model, corepressor binding to Mediator components inhibits them from forming a fully active Mediator complex, Polymerase II recruitment and promoter escape, the main roles of the Mediator complex (Petrenko et al., 2017).

TPL interaction with MED21 has implications for the dynamics of transcriptional activation. By stabilizing the Mediator complex, TPL (and by extension Tup1) may create a 'pre-paused' state that allows rapid recruitment of Pol-II and activation once TPL is removed. Alternatively, TPL could allow for recruitment of a poised or paused Pol-II, allowing for rapid activation (and re-activation) of a repressed locus. Support for this idea comes from the genome-wide correlation between Groucho corepressor binding and polymerase pausing in *Drosophila* (Kaul et al., 2014). However, in non-metazoan lineages (i.e. plants and yeast) the existence of bona fide pausing is disputed, mainly due to the absence of the pausing regulator Negative Elongation Factor complex (NELF, (Gaertner and Zeitlinger, 2014)). One possibility is that plants and yeast have an alternative or more primitive form of pausing that is NELF-independent. Support for this idea comes from studies of *Arabidopsis* where Pol-II was found to be markedly enriched at the five-prime ends of genes, the same pattern seen with pausing (Zhu et al., 2018). In yeast, Tup1 has been implicated in a form of transcriptional memory that involves recruiting a poised form of preinitiation Pol-II to allow rapid reactivation of genes involved in sugar utilization (Sood et al., 2017).

Multiple points of contact likely exist between the Mediator complex and other parts of the transcriptional machinery in both transcriptionally repressed and active states. For auxin response, specifically, there are several lines of evidence to support this model, including documented association between the structural backbone of Mediator, MED14, and activated and repressed auxin loci in *Arabidopsis* (Ito et al., 2016). In addition, MED12 and MED13 are required for auxin-responsive gene expression in the root, and MED12 acts upstream of AUX1 in the root growth response to sugar (Raya-González et al., 2018). MED18 in the head module represses auxin signaling and positively regulates the viability of the root meristem (Raya-González et al., 2018). PFT1/MED25 regulates auxin transport and response in the root (Raya-González et al., 2014). MED7, MED21's partner protein in the hinge domain, is required for normal root development and loss of MED7 function impacts expression of auxin signaling components (Kumar et al., 2018). Previous research identified the Mediator CDK8 subunit, specifically MED13 (MAB2), as an interactor with the full-length TPL protein (Ito et al., 2016). We could not observe interaction between the N-terminal domain of TPL and AtMED13, AtCYC8, or AtCYCC (Figure Supplement 2), suggesting that any direct interactions occur outside the N188 fragment. As suggested by Ito and colleagues (Ito et al., 2016) and supported by our synthetic system, auxin-induced removal of TPL is sufficient to induce changes in the composition of the Mediator complex, facilitating both rapid activation and rapid return to a repressed basal state.

While TPL can form higher order multimer states that may have altered repression dynamics, multimerization is not required for repression in our experiments. Formation of tetrameric TPL has been suspected to increase repression of target genes, either by increasing the local concentration of TPL for interaction with partner

proteins, or by allowing higher-order chromatin compaction for example by physical interaction with histone tails (Ma et al., 2017). The loss of dimerization through the CRA domain (what we call LDimer in this study) was found to have no effect on transcriptional repression of the DR5 promoter in protoplasts (Martin-Arevalillo et al., 2017). Similarly, we found that LDimer and Monomer forms of TPL were effective corepressors in yeast and in plants. One caveat from our data is that we tested everything in the context of the auxin response pathway. It is entirely possible that other TPL-regulated loci that are not auxin-regulated have different requirements.

Rapid state switching triggered by small molecule-induced protein degradation is among the many properties of the auxin system that make it an attractive candidate for continued prospecting for new parts to use in synthetic biology applications. The clustering of TPL and TBL1 with LisH domains from diverse phyla (Figure 6, Figure 6 – Figure supplement 1), in combination with *At*ARC^{Sc}, should allow for rapid assembly of a large set of repression domains with diverse sequences and a range of strengths and dynamic properties. Once a core set of repression domains has been identified, they can likely can be further optimized for a given specification (e.g., *in vivo* computation such as in (Gander et al., 2017)). Our current tools to repress transcriptional output in plants are limited, and frequently depend on recruitment of endogenous TPL/TPR complexes to a synthetic EAR domain (SRDX - (Hiratsu et al., 2003)) or fusion of the TPL N-terminal domain to transcription factors (HACR - (Khakhar et al., 2018)). The development of a graded set of repression domains that act orthogonally to the endogenous TPL/TPR corepressors will allow an expansion of the synthetic circuitry possible in plants.

Methods

Cloning

Construction of TPL-IAA3 and TPL-IAA14 fusion proteins were performed as described in (Pierre-Jerome et al., 2014). Variant and deletion constructs were created using PCR-mediated site directed mutagenesis. Site-directed mutagenesis primers were designed using NEBasechanger and implemented through Q5® Site-Directed Mutagenesis (NEB, Cat #E0554S). TPL interactor genes were amplified as cDNAs from wild type Col-0 RNA using reverse transcriptase (SuperScript™ IV Reverse Transcriptase, Invitrogen) and gene specific primers from IDT (Coralville, Iowa), followed by amplification with Q5 polymerase (NEB). These cDNAs were subsequently cloned into Plasmids for cytoSUS using a Gibson approach (Gibson et al., 2009), through the Aquarium Biofabrication facility (Ben Keller et al., 2019). The coding sequence of the genes of interest were confirmed by sequencing (Genewiz; South Plainfield, NJ). For UAS driven constructs, the TPLN188-IAA14 coding sequence was amplified with primers containing engineered BsaI sites and introduced into the pGII backbone with the UAS promoter and RBSC terminator (Siligato et al., 2016) using Golden Gate cloning (Weber et al., 2011). Subsequent mutations were performed on this backbone using PCR-mediated site directed mutagenesis (See above). Construction of C-terminal 2xFRB fusions for Anchor Away were constructed as described in (Haruki et al., 2008). Inducible MED21 was constructed as described in (McIsaac et al., 2013).

Flow Cytometry

Fluorescence measurements were taken using a Becton Dickinson (BD) special order cytometer with a 514-nm laser exciting fluorescence that is cutoff at 525 nm prior to photomultiplier tube collection (BD, Franklin Lakes, NJ). Events were annotated, subset to singlet yeast using the flowTime R package (Wright et al., 2019). A total of 10,000 - 20,000 events above a 400,000 FSC-H threshold (to exclude debris) were collected for each sample and data exported as FCS 3.0 files for processing using the flowCore R software package and custom R scripts (Supplemental File 1, (Havens et al., 2012; Pierre-Jerome et al., 2017)). Data from at least two independent replicates were combined and plotted in R (ggplots2).

Yeast Methods

Standard yeast drop-out and yeast extract–peptone–dextrose plus adenine (YPAD) media were used, with care taken to use the same batch of synthetic complete (SC) media for related experiments. A standard lithium acetate protocol (Gietz and Woods, 2002) was used for transformations of digested plasmids. All cultures were grown at 30°C with shaking at 220 rpm. Anchor-Away approaches were followed as described in

(Haruki et al., 2008), and anchor away strains were obtained from EURO-SCARF (euroscarf.de). Endogenous genomic fusions of ScMed21-FRB were designed by fusing MED21 homology to the pFA6a-FRB-KanMX6 plasmid for chromosomal integration into the parental anchor away strain as in (Petrenko et al., 2017), selectable through G418 resistance (G418, Geneticin, Thermo Fisher Scientific). Tup1-FRB and Cyc8-FRB were constructed as described in (Wong and Struhl, 2011). SLARC construction required a redesign of promoters and terminators used in the AtARCSc to eliminate any repetitive DNA sequences (See Figure 4 – Figure Supplement 1), using a Golden Gate cloning approach into level 1 vectors. Subsequent assembly of individual transcriptional units into a larger plasmid utilized VEGAS assembly which was performed as described in (Mitchell et al., 2015). To create an acceptor plasmid for the assembled transcriptional units, we synthesized a custom vector containing VA1 and VA2 homology sites for recombination (Twist Bioscience, South San Francisco, CA). In between these sites we incorporated a pLac:mRFP cassette to allow identification of uncut destination plasmid in *E. coli*, flanked by EcoRI sites for linearization. Finally, the CEN6/ARSH4 was transferred from pRG215 (Addgene #64525) into the acceptor plasmid by Golden Gate reaction using designed BsmBI sites engineered into the acceptor plasmid and the primers used to amplify the CEN/ARS (See Figure 4 – Figure Supplement 1). For the cytoplasmic split-ubiquitin protein-protein interaction system, bait and prey constructs were created using the plasmids pMetOYC and pNX32, respectively (Addgene, https://www.addgene.org/Christopher_Grefen/). Interaction between bait and prey proteins were evaluated using a modified version of the split ubiquitin technique (Asseck and Grefen, 2018). After two days of growth on control and selection plates, images were taken using a flatbed scanner (Epson America, Long Beach, CA). Inducible ScMed21 strains (iMed21) were grown overnight, and then diluted back to 100 events per microliter as determined by flow cytometry and grown at 30C with 250rpm in a deepwell 96-well plate format. Strains were supplemented with β-estradiol (20μM) for 4 hours followed by Rapamycin addition. Samples were analyzed by flow cytometry throughout these growth experiments.

Western Blot

Yeast cultures that had been incubated overnight in synthetic complete (SC) media were diluted to OD600 = 0.6 and incubated until cultures reached OD600 ~1. Cells were harvested by centrifugation. Cells were lysed by vortexing for 5 min in the presence of 200 µl of 0.5-mm diameter acid washed glass beads and 200 µl SUMEB buffer (1% SDS, 8 M urea, 10 mM MOPS pH 6.8, 10 mM EDTA, 0.01% bromophenol blue, 1mM PMSF) per one OD unit of original culture. Lysates were then incubated at 65° for 10 min and cleared by centrifugation prior to electrophoresis and blotting. Antibodies: Anti-HA-HRP (REF-12013819001, Clone 3F10, Roche/Millipore Sigma, St. Louis, MO), Anti-FLAG (F3165, Monoclonal ANTI-FLAG® M2, Millipore Sigma, St.

Louis, MO), Anti-FRB (ALX-215-065-1, Enzo Life Sciences, Farmingdale, NY, (Haruki et al., 2008)).

Protein expression and purification

All multimer deficient TPL proteins were expressed in *Escherichia coli* Rosetta 2 strain. Bacteria cultures were grown at 37ºC until they achieved an OD^{600}nm of 0.6-0.9. Protein expression was induced with isopropyl-β-D-1-thyogalactopiranoside (IPTG) at a final concentration of 400 µM at 18 °C overnight. Bacteria cultures were centrifuged and the pellets were resuspended in the buffer A (CAPS 200 mM pH 10.5, NaCl 500 mM, TCEP 1 mM), where cells were lysed by sonication. His-tagged AtTPL188 (wt and mutants) bacteria pellets were resuspended in buffer A with EDTA-free antiprotease (Roche). The soluble fractions recovered after sonication were passed through a Ni-sepharose (GE Healthcare) column previously washed with buffer A and the bound proteins were eluted with buffer A with 300 mM imidazole. A second purification step was carried out on Gel filtration Superdex 200 10/300 GL (GE Healthcare) equilibrated with buffer A.

Protein Alignments

The TPL LisH domain was added to an alignment of seed sequences for PFAM08513 containing 50 seed sequences (the curated alignment from which the HMM for the family is built). These were aligned using CLC Sequence Viewer 7, a tree was constructed using a Neighbor Joining method, and bootstrap analysis performed with 10,000 replicates.

Plant growth

Agrobacterium mediated transient transformation of *Nicotiana benthamiana* was performed as per (Yang et al., 2000). 5 ml cultures of agrobacterium strains were grown overnight at 30C shaking at 220rpm, pelleted and incubated in MMA media (10 mM MgCl2, 10 mM MES pH 5.6, 100 µM acetosyringone) for 3 hours at room temperature with rotation. Strain density was normalized to an OD600 of 1 for each strain in the final mixture of strains before injection into tobacco leaves. Leaves were removed, and 8 different regions were excised using a hole punch, placed into a 96-well microtiter plate with 100µl of water. Each leaf punch was scanned in a 4x4 grid for yellow and red fluorescence using a plate scanner (Tecan Spark, Tecan Trading AG, Switzerland). Fluorescence data was quantified and plotted in R (ggplots). For *Arabidopsis thaliana* experiments, J0121 was introgressed eight times into Col-0 accession from the C24 accession, rigorously checked to ensure root growth was comparable to Col-0 before use. UAS-TPL-$IAA14^{mED}$ constructs were introduced to J0121 introgression lines by floral dip method (Clough and Bent, 1998). T1 seedlings were selected on 0.5X LS (Caisson Laboratories, Smithfield, UT) + 25µg/ml Hygromycin B (company) + 0.8% phytoagar (Plantmedia; Dublin, OH). Plates were stratified for 2 days, exposed to light

for 6 h, and then grown in the dark for 3 d following a modification of the method of (Harrison et al., 2006). Hygromycin resistant seedlings were identified by their long hypocotyl, enlarged green leaves and long root. Transformants were transferred by hand to fresh 0.5X LS plates + 0.8% Bacto agar (Thermo Fisher Scientific) and grown vertically for 14 days at 22°C. Plates were scanned on a flatbed scanner (Epson America, Long Beach, CA) at day 14. *slr* seeds were obtained from the Arabidopsis Biological Resource Center (Columbus, OH).

Data Submissions

All flow cytometry data will be deposited at https://flowrepository.org/. All plasmids will be deposited through Addgene at https://www.addgene.org/Jennifer_Nemhauser/.

Acknowledgements

We would like to thank Prof. Jef Boeke for kindly providing VEGAS adaptor and regulatory element plasmids; Dr. Jennifer Brophy and Prof. José Dinneny for kindly providing the pUBQ10:GAL4:VP16 plasmid; and Prof. Grant Brown and Prof. Maitreya Dunham for advice on yeast genetics and approaches. We thank members of the Nemhauser group including Amy Lanctot, Romi Ramos, Eric Yang, and Dr. Sarah Guiziou for constructive discussions and comments on this manuscript. We also thank Morgan Hamm for the custom R script used here to analyze anchor away plates.

Funding

National Institutes of Health (NIH): ARL, SJS, JEZ, MZ & JLN R01- GM107084
Howard Hughes Medical Institute (HHMI): ARL, SJS, JEZ, MZ & JLN - Faculty Scholar Award. Ning Zheng is a Howard Hughes Medical Institute Investigator. ARL is supported by the Simons Foundation through the Life Science Research Foundation.

References

Adams GE, Chandru A, Cowley SM. 2018. Co-repressor, co-activator and general transcription factor: the many faces of the Sin3 histone deacetylase (HDAC) complex. *Biochem J* **475**:3921–3932. doi:10.1042/BCJ20170314

Agarwal M, Kumar P, Mathew SJ. 2015. The Groucho/Transducin-like enhancer of split protein family in animal development. *IUBMB Life* **67**:472–481. doi:10.1002/iub.1395

Asseck LY, Grefen C. 2018. Detecting Interactions of Membrane Proteins: The Split-Ubiquitin System. *Methods Mol Biol Clifton NJ* **1794**:49–60. doi:10.1007/978-1-4939-7871-7_4

Baumli S, Hoeppner S, Cramer P. 2005. A Conserved Mediator Hinge Revealed in the Structure of the MED7·MED21 (Med7·Srb7) Heterodimer. *J Biol Chem* **280**:18171–18178. doi:10.1074/jbc.M413466200

Ben Keller, Justin Vrana, Abraham Miller, Garrett Newman, Eric Klavins. 2019. Aquarium: The Laboratory Operating System. Zenodo. doi:10.5281/zenodo.2535715

Bourbon H-M. 2008. Comparative genomics supports a deep evolutionary origin for the large, four-module transcriptional mediator complex. *Nucleic Acids Res* **36**:3993–4008. doi:10.1093/nar/gkn349

Brand AH, Perrimon N. 1993. Targeted gene expression as a means of altering cell fates and generating dominant phenotypes. *Dev Camb Engl* **118**:401–415.

Busch W, Miotk A, Ariel FD, Zhao Z, Forner J, Daum G, Suzaki T, Schuster C, Schultheiss SJ, Leibfried A, Haubeiss S, Ha N, Chan RL, Lohmann JU. 2010. Transcriptional control of a plant stem cell niche. *Dev Cell* **18**:849–861. doi:10.1016/j.devcel.2010.03.012

Causier B, Ashworth M, Guo W, Davies B. 2012. The TOPLESS interactome: a framework for gene repression in Arabidopsis. *Plant Physiol* **158**:423–438. doi:10.1104/pp.111.186999

Chen G, Courey AJ. 2000. Groucho/TLE family proteins and transcriptional repression. *Gene* **249**:1–16. doi:10.1016/s0378-1119(00)00161-x

Clough SJ, Bent AF. 1998. Floral dip: a simplified method for Agrobacterium-mediated transformation of Arabidopsis thaliana. *Plant J Cell Mol Biol* **16**:735–743.

Collins J, O'Grady K, Chen S, Gurley W. 2019. The C-terminal WD40 repeats on the TOPLESS co-repressor function as a protein–protein interaction surface. *Plant Mol Biol* **100**:47–58. doi:10.1007/s11103-019-00842-w

Delto CF, Heisler FF, Kuper J, Sander B, Kneussel M, Schindelin H. 2015. The LisH motif of muskelin is crucial for oligomerization and governs intracellular localization. *Struct Lond Engl 1993* **23**:364–373. doi:10.1016/j.str.2014.11.016

Dolan WL, Chapple C. 2017. Conservation and Divergence of Mediator Structure and Function: Insights from Plants. *Plant Cell Physiol* **58**:4–21. doi:10.1093/pcp/pcw176

Flanagan PM, Kelleher RJ, Sayre MH, Tschochner H, Kornberg RD. 1991. A mediator required for activation of RNA polymerase II transcription in vitro. *Nature* **350**:436–438. doi:10.1038/350436a0

Flowers EB, Poole RJ, Tursun B, Bashllari E, Pe'er I, Hobert O. 2010. The Groucho ortholog UNC-37 interacts with the short Groucho-like protein LSY-22 to control developmental decisions in C. elegans. *Dev Camb Engl* **137**:1799–1805. doi:10.1242/dev.046219

Fukaki H, Tameda S, Masuda H, Tasaka M. 2002. Lateral root formation is blocked by a gain-of-function mutation in the SOLITARY-ROOT/IAA14 gene of Arabidopsis. *Plant J Cell Mol Biol* **29**:153–168.

Gaertner B, Zeitlinger J. 2014. RNA polymerase II pausing during development. *Development* **141**:1179–1183. doi:10.1242/dev.088492

Gander MW, Vrana JD, Voje WE, Carothers JM, Klavins E. 2017. Digital logic circuits in yeast with CRISPR-dCas9 NOR gates. *Nat Commun* **8**:15459. doi:10.1038/ncomms15459

Gasperowicz M, Otto F. 2005. Mammalian Groucho homologs: redundancy or specificity? *J Cell Biochem* **95**:670–687. doi:10.1002/jcb.20476

Gibson DG, Young L, Chuang R-Y, Venter JC, Hutchison CA, Smith HO. 2009. Enzymatic assembly of DNA molecules up to several hundred kilobases. *Nat Methods* **6**:343–345. doi:10.1038/nmeth.1318

Gietz RD, Woods RA. 2002. Transformation of yeast by lithium acetate/single-stranded carrier DNA/polyethylene glycol method. *Methods Enzymol* **350**:87–96. doi:10.1016/s0076-6879(02)50957-5

Gonzalez N, Pauwels L, Baekelandt A, De Milde L, Van Leene J, Besbrugge N, Heyndrickx KS, Cuéllar Pérez A, Durand AN, De Clercq R, Van De Slijke E, Vanden Bossche R, Eeckhout D, Gevaert K, Vandepoele K, De Jaeger G, Goossens A, Inzé D. 2015. A Repressor Protein Complex Regulates Leaf Growth in Arabidopsis. *Plant Cell* **27**:2273–2287. doi:10.1105/tpc.15.00006

Grbavec D, Lo R, Liu Y, Stifani S. 1998. Transducin-like Enhancer of split 2, a mammalian homologue of Drosophila Groucho, acts as a transcriptional repressor, interacts with Hairy/Enhancer of split proteins, and is expressed during neuronal development. *Eur J Biochem* **258**:339–349.

Gromöller A, Lehming N. 2000. Srb7p is a physical and physiological target of Tup1p. *EMBO J* **19**:6845–6852. doi:10.1093/emboj/19.24.6845

Hallberg M, Hu G-Z, Tronnersjö S, Shaikhibrahim Z, Balciunas D, Björklund S, Ronne H. 2006. Functional and physical interactions within the middle domain of the yeast mediator. *Mol Genet Genomics MGG* **276**:197–210. doi:10.1007/s00438-006-0135-7

Hamm MO, Moss BL, Leydon AR, Gala HP, Lanctot A, Ramos R, Klaeser H, Lemmex AC, Zahler ML, Nemhauser JL, Wright RC. 2019. Accelerating structure-function mapping using the ViVa webtool to mine natural variation. *Plant Direct* **3**:e00147. doi:10.1002/pld3.147

Haruki H, Nishikawa J, Laemmli UK. 2008. The anchor-away technique: rapid, conditional establishment of yeast mutant phenotypes. *Mol Cell* **31**:925–932. doi:10.1016/j.molcel.2008.07.020

Havens KA, Guseman JM, Jang SS, Pierre-Jerome E, Bolten N, Klavins E, Nemhauser JL. 2012. A synthetic approach reveals extensive tunability of auxin signaling. *Plant Physiol* **160**:135–142. doi:10.1104/pp.112.202184

Hiratsu K, Matsui K, Koyama T, Ohme-Takagi M. 2003. Dominant repression of target genes by chimeric repressors that include the EAR motif, a repression domain, in Arabidopsis. *Plant J* **34**:733–739. doi:10.1046/j.1365-313X.2003.01759.x

Ito J, Fukaki H, Onoda M, Li L, Li C, Tasaka M, Furutani M. 2016. Auxin-dependent compositional change in Mediator in ARF7- and ARF19-mediated transcription. *Proc Natl Acad Sci U S A* **113**:6562–6567. doi:10.1073/pnas.1600739113

Kagale S, Links MG, Rozwadowski K. 2010. Genome-wide analysis of ethylene-responsive element binding factor-associated amphiphilic repression motif-containing transcriptional regulators in Arabidopsis. *Plant Physiol* **152**:1109–1134. doi:10.1104/pp.109.151704

Kaul A, Schuster E, Jennings BH. 2014. The Groucho co-repressor is primarily recruited to local target sites in active chromatin to attenuate transcription. *PLoS Genet* **10**:e1004595. doi:10.1371/journal.pgen.1004595

Ke J, Ma H, Gu X, Thelen A, Brunzelle JS, Li J, Xu HE, Melcher K. 2015. Structural basis for recognition of diverse transcriptional repressors by the TOPLESS family of corepressors. *Sci Adv* **1**:e1500107. doi:10.1126/sciadv.1500107

Khakhar A, Leydon AR, Lemmex AC, Klavins E, Nemhauser JL. 2018. Synthetic hormone-responsive transcription factors can monitor and re-program plant development. *eLife* **7**. doi:10.7554/eLife.34702

Kim MH, Cooper DR, Oleksy A, Devedjiev Y, Derewenda U, Reiner O, Otlewski J, Derewenda ZS. 2004. The Structure of the N-Terminal Domain of the Product of the Lissencephaly

Gene Lis1 and Its Functional Implications. *Structure* **12**:987–998. doi:10.1016/j.str.2004.03.024

Kim YJ, Björklund S, Li Y, Sayre MH, Kornberg RD. 1994. A multiprotein mediator of transcriptional activation and its interaction with the C-terminal repeat domain of RNA polymerase II. *Cell* **77**:599–608. doi:10.1016/0092-8674(94)90221-6

Krogan NT, Hogan K, Long JA. 2012. APETALA2 negatively regulates multiple floral organ identity genes in Arabidopsis by recruiting the co-repressor TOPLESS and the histone deacetylase HDA19. *Dev Camb Engl* **139**:4180–4190. doi:10.1242/dev.085407

Kumar KRR, Blomberg J, Björklund S. 2018. The MED7 subunit paralogs of Mediator function redundantly in development of etiolated seedlings in Arabidopsis. *Plant J* **96**:578–594. doi:10.1111/tpj.14052

Laplaze L, Parizot B, Baker A, Ricaud L, Martinière A, Auguy F, Franche C, Nussaume L, Bogusz D, Haseloff J. 2005. GAL4-GFP enhancer trap lines for genetic manipulation of lateral root development in Arabidopsis thaliana. *J Exp Bot* **56**:2433–2442. doi:10.1093/jxb/eri236

Lee JE, Golz JF. 2012. Diverse roles of Groucho/Tup1 co-repressors in plant growth and development. *Plant Signal Behav* **7**:86–92. doi:10.4161/psb.7.1.18377

Lee M, Chatterjee S, Struhl K. 2000. Genetic analysis of the role of Pol II holoenzyme components in repression by the Cyc8-Tup1 corepressor in yeast. *Genetics* **155**:1535–1542.

Liu X, Galli M, Camehl I, Gallavotti A. 2019. RAMOSA1 ENHANCER LOCUS2-Mediated Transcriptional Repression Regulates Vegetative and Reproductive Architecture. *Plant Physiol* **179**:348–363. doi:10.1104/pp.18.00913

Liu Z, Karmarkar V. 2008. Groucho/Tup1 family co-repressors in plant development. *Trends Plant Sci* **13**:137–144. doi:10.1016/j.tplants.2007.12.005

Long JA, Ohno C, Smith ZR, Meyerowitz EM. 2006. TOPLESS regulates apical embryonic fate in Arabidopsis. *Science* **312**:1520–1523. doi:10.1126/science.1123841

Ma H, Duan J, Ke J, He Y, Gu X, Xu T-H, Yu H, Wang Y, Brunzelle JS, Jiang Y, Rothbart SB, Xu HE, Li J, Melcher K. 2017. A D53 repression motif induces oligomerization of TOPLESS corepressors and promotes assembly of a corepressor-nucleosome complex. *Sci Adv* **3**:e1601217. doi:10.1126/sciadv.1601217

Maji S, Dahiya P, Waseem M, Dwivedi N, Bhat DS, Dar TH, Thakur JK. 2019. Interaction map of Arabidopsis Mediator complex expounding its topology. *Nucleic Acids Res* **47**:3904–3920. doi:10.1093/nar/gkz122

Malik N, Agarwal P, Tyagi A. 2017. Emerging functions of multi-protein complex Mediator with special emphasis on plants. *Crit Rev Biochem Mol Biol* **52**:475–502. doi:10.1080/10409238.2017.1325830

Martin-Arevalillo R, Nanao MH, Larrieu A, Vinos-Poyo T, Mast D, Galvan-Ampudia C, Brunoud G, Vernoux T, Dumas R, Parcy F. 2017. Structure of the Arabidopsis TOPLESS corepressor provides insight into the evolution of transcriptional repression. *Proc Natl Acad Sci U S A*. doi:10.1073/pnas.1703054114

Martin-Arevalillo R, Thévenon E, Jégu F, Vinos-Poyo T, Vernoux T, Parcy F, Dumas R. 2019. Evolution of the Auxin Response Factors from charophyte ancestors. *PLoS Genet* **15**:e1008400. doi:10.1371/journal.pgen.1008400

Matsumura H, Kusaka N, Nakamura T, Tanaka N, Sagegami K, Uegaki K, Inoue T, Mukai Y. 2012. Crystal structure of the N-terminal domain of the yeast general corepressor Tup1p and its functional implications. *J Biol Chem* **287**:26528–26538. doi:10.1074/jbc.M112.369652

Mayer KS, Chen X, Sanders D, Chen J, Jiang J, Nguyen P, Scalf M, Smith LM, Zhong X. 2019. HDA9-PWR-HOS15 Is a Core Histone Deacetylase Complex Regulating Transcription and Development. *Plant Physiol* **180**:342–355. doi:10.1104/pp.18.01156

McIsaac RS, Oakes BL, Wang X, Dummit KA, Botstein D, Noyes MB. 2013. Synthetic gene expression perturbation systems with rapid, tunable, single-gene specificity in yeast. *Nucleic Acids Res* **41**:e57. doi:10.1093/nar/gks1313

Mitchell LA, Chuang J, Agmon N, Khunsriraksakul C, Phillips NA, Cai Y, Truong DM, Veerakumar A, Wang Y, Mayorga M, Blomquist P, Sadda P, Trueheart J, Boeke JD. 2015. Versatile genetic assembly system (VEGAS) to assemble pathways for expression in S. cerevisiae. *Nucleic Acids Res* **43**:6620–6630. doi:10.1093/nar/gkv466

Mottis A, Mouchiroud L, Auwerx J. 2013. Emerging roles of the corepressors NCoR1 and SMRT in homeostasis. *Genes Dev* **27**:819–835. doi:10.1101/gad.214023.113

Oberoi J, Fairall L, Watson PJ, Yang J-C, Czimmerer Z, Kampmann T, Goult BT, Greenwood JA, Gooch JT, Kallenberger BC, Nagy L, Neuhaus D, Schwabe JWR. 2011. Structural basis for the assembly of the SMRT/NCoR core transcriptional repression machinery. *Nat Struct Mol Biol* **18**:177–184. doi:10.1038/nsmb.1983

Papamichos-Chronakis M, Conlan RS, Gounalaki N, Copf T, Tzamarias D. 2000. Hrs1/Med3 is a Cyc8-Tup1 corepressor target in the RNA polymerase II holoenzyme. *J Biol Chem* **275**:8397–8403. doi:10.1074/jbc.275.12.8397

Perissi V, Jepsen K, Glass CK, Rosenfeld MG. 2010. Deconstructing repression: evolving models of co-repressor action. *Nat Rev Genet* **11**:109–123. doi:10.1038/nrg2736

Petrenko N, Jin Y, Wong KH, Struhl K. 2017. Evidence that Mediator is essential for Pol II transcription, but is not a required component of the preinitiation complex in vivo. *eLife* **6**:e28447. doi:10.7554/eLife.28447

Pierre-Jerome E, Jang SS, Havens KA, Nemhauser JL, Klavins E. 2014. Recapitulation of the forward nuclear auxin response pathway in yeast. *Proc Natl Acad Sci U S A* **111**:9407–9412. doi:10.1073/pnas.1324147111

Pierre-Jerome E, Wright RC, Nemhauser JL. 2017. Characterizing Auxin Response Circuits in Saccharomyces cerevisiae by Flow Cytometry. *Methods Mol Biol Clifton NJ* **1497**:271–281. doi:10.1007/978-1-4939-6469-7_22

Raya-González J, Oropeza-Aburto A, López-Bucio JS, Guevara-García ÁA, de Veylder L, López-Bucio J, Herrera-Estrella L. 2018. MEDIATOR18 influences Arabidopsis root architecture, represses auxin signaling and is a critical factor for cell viability in root meristems. *Plant J Cell Mol Biol* **96**:895–909. doi:10.1111/tpj.14114

Raya-González J, Ortiz-Castro R, Ruíz-Herrera LF, Kazan K, López-Bucio J. 2014. PHYTOCHROME AND FLOWERING TIME1/MEDIATOR25 Regulates Lateral Root Formation via Auxin Signaling in Arabidopsis. *Plant Physiol* **165**:880–894. doi:10.1104/pp.114.239806

Samanta S, Thakur JK. 2015. Importance of Mediator complex in the regulation and integration of diverse signaling pathways in plants. *Front Plant Sci* **6**:757. doi:10.3389/fpls.2015.00757

Sato S, Tomomori-Sato C, Tsai K-L, Yu X, Sardiu M, Saraf A, Washburn MP, Florens L, Asturias FJ, Conaway RC, Conaway JW. 2016. Role for the MED21-MED7 Hinge in Assembly of the Mediator-RNA Polymerase II Holoenzyme. *J Biol Chem* **291**:26886–26898. doi:10.1074/jbc.M116.756098

Schreiber-Agus N, Chin L, Chen K, Torres R, Rao G, Guida P, Skoultchi AI, DePinho RA. 1995. An amino-terminal domain of Mxi1 mediates anti-Myc oncogenic activity and interacts with a homolog of the yeast transcriptional repressor SIN3. *Cell* **80**:777–786.

Schuster-Böckler B, Schultz J, Rahmann S. 2004. HMM Logos for visualization of protein families. *BMC Bioinformatics* **5**:7. doi:10.1186/1471-2105-5-7

Siligato R, Wang X, Yadav SR, Lehesranta S, Ma G, Ursache R, Sevilem I, Zhang J, Gorte M, Prasad K, Wrzaczek M, Heidstra R, Murphy A, Scheres B, Mähönen AP. 2016. MultiSite Gateway-Compatible Cell Type-Specific Gene-Inducible System for Plants. *Plant Physiol* **170**:627–641. doi:10.1104/pp.15.01246

Sood V, Cajigas I, D'Urso A, Light WH, Brickner JH. 2017. Epigenetic Transcriptional Memory of GAL Genes Depends on Growth in Glucose and the Tup1 Transcription Factor in Saccharomyces cerevisiae. *Genetics* **206**:1895–1907. doi:10.1534/genetics.117.201632

Ulmasov T, Hagen G, Guilfoyle TJ. 1997. ARF1, a transcription factor that binds to auxin response elements. *Science* **276**:1865–1868. doi:10.1126/science.276.5320.1865

Weber E, Engler C, Gruetzner R, Werner S, Marillonnet S. 2011. A Modular Cloning System for Standardized Assembly of Multigene Constructs. *PLOS ONE* **6**:e16765. doi:10.1371/journal.pone.0016765

Wong KH, Struhl K. 2011. The Cyc8-Tup1 complex inhibits transcription primarily by masking the activation domain of the recruiting protein. *Genes Dev* **25**:2525–2539. doi:10.1101/gad.179275.111

Wong MM, Guo C, Zhang J. 2014. Nuclear receptor corepressor complexes in cancer: mechanism, function and regulation. *Am J Clin Exp Urol* **2**:169–187.

Wright RC, Bolten N, Pierre-Jerome E. 2019. flowTime: Annotation and analysis of biological dynamical systems using flow cytometry. Bioconductor version: Release (3.10). doi:10.18129/B9.bioc.flowTime

Yang Y, Li R, Qi M. 2000. In vivo analysis of plant promoters and transcription factors by agroinfiltration of tobacco leaves. *Plant J* **22**:543–551. doi:10.1046/j.1365-313x.2000.00760.x

Zhang Y, Gao S, Wang Z. 2010. Structural and functional analysis of amino-terminal enhancer of split in androgen-receptor-driven transcription. *Biochem J* **427**:499–511. doi:10.1042/BJ20091631

Zhang Z, Reese JC. 2004. Redundant Mechanisms Are Used by Ssn6-Tup1 in Repressing Chromosomal Gene Transcription in Saccharomyces cerevisiae. *J Biol Chem* **279**:39240–39250. doi:10.1074/jbc.M407159200

Zhu J, Jeong JC, Zhu Y, Sokolchik I, Miyazaki S, Zhu J-K, Hasegawa PM, Bohnert HJ, Shi H, Yun D-J, Bressan RA. 2008. Involvement of Arabidopsis HOS15 in histone deacetylation and cold tolerance. *Proc Natl Acad Sci* **105**:4945–4950. doi:10.1073/pnas.0801029105

Zhu J, Liu M, Liu X, Dong Z. 2018. RNA polymerase II activity revealed by GRO-seq and pNET-seq in Arabidopsis. *Nat Plants* **4**:1112–1123. doi:10.1038/s41477-018-0280-0

Supplemental Figures

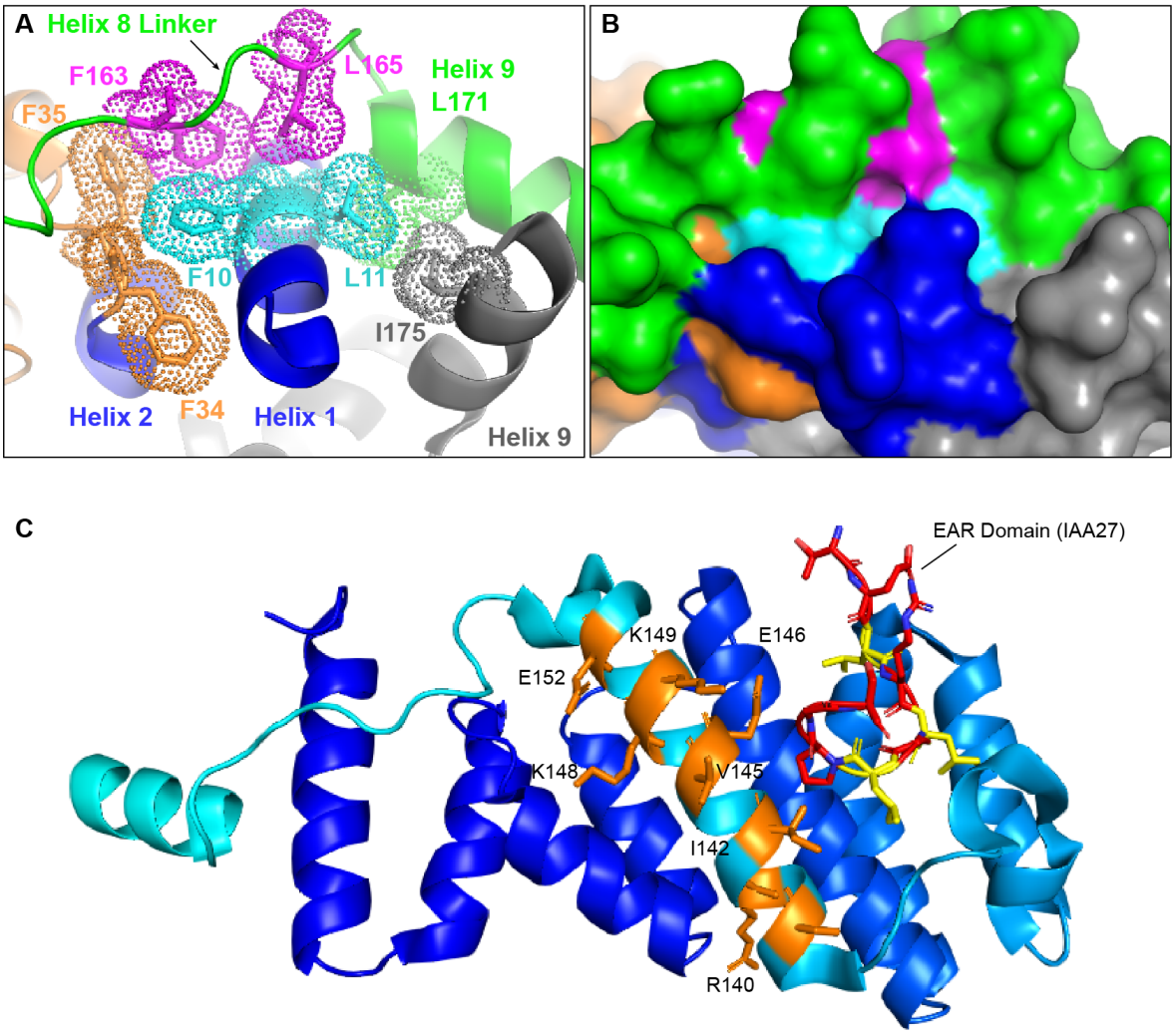

Figure 2 – Figure Supplement 1. A. The position of the hydrophobic residues in helix one that allow confer auxin sensitivity to the *At*ARC^{Sc}. In the context of the full-length N-terminus of TPL, F10 and its hydrophobic neighbor L11 sit underneath the linker that connects Helix 8 to Helix 9, interacting with inward-facing hydrophobic residues F163 and L165. Further stabilization of F10 likely comes from F34 and F35 in the CTLH domain, while L11 is likely stabilized by L171 from Intra-Helix 9 interactions, and I175 from inter-Helix 9 interactions. **B.** The surface rendering of this region helps visualize the buried nature of these residues in the full-length structure. The second monomer of TPL bound at the LisH-Helix 9 interface is colored gray. **C**. MED21 binding and EAR motif binding utilize an overlapping interaction interface. One Monomer of TPL is shown in a gradient of Blue, with the EAR motif of AtIAA27 (red) bound in the groove created by helices 5-8, with the conserved Lysines (LxLxL – yellow). The amino acids mutated in helix 8 that affect repression and MED21 binding are colored in gold. PDB 5NQV.

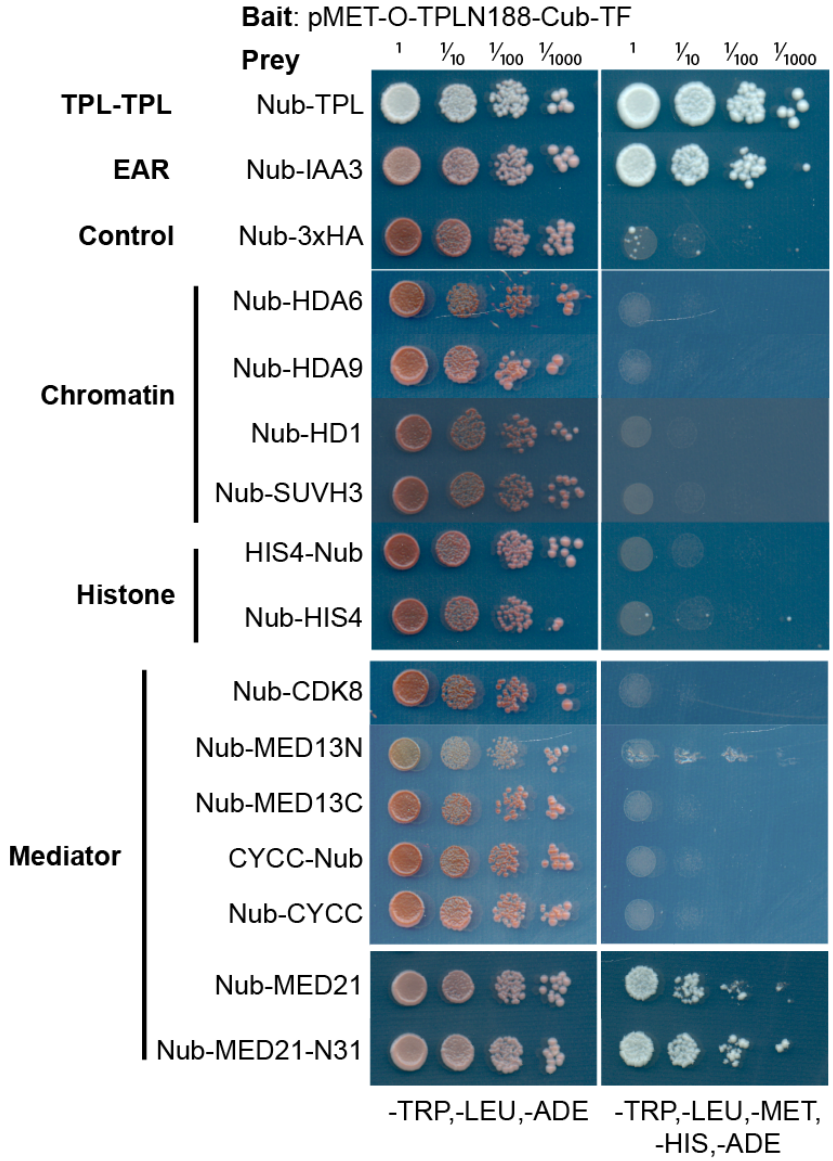

Figure 3 – Figure Supplement 1. TPL-N terminal domain (TPLN188) interacts with the N-terminus of AtMED21. Identifying TPL-N terminal domain interactor proteins through cytoplasmic split ubiquitin protein interaction assay. We tested the N-terminal and C-terminal portions of MED13 separately and divided the coding sequence at amino acid 967 (MED13N = aa1-967, MED13C = aa968-1908). Each bait tested is the *Arabidopsis* homolog cloned from cDNA from the Col-0 accession, with the exception of MED13, which was synthesized via Twist (https://www.twistbioscience.com/). Interaction of bait and prey proteins reconstitute split ubiquitin, release a synthetic transcription factor that allows growth on media lacking Histidine and Adenine. The relative position of the N-terminal portion of ubiquitin (Nub) is indicated for each bait protein. Plates were scanned at 3 days after plating to allow weaker interactions to develop if they were present.

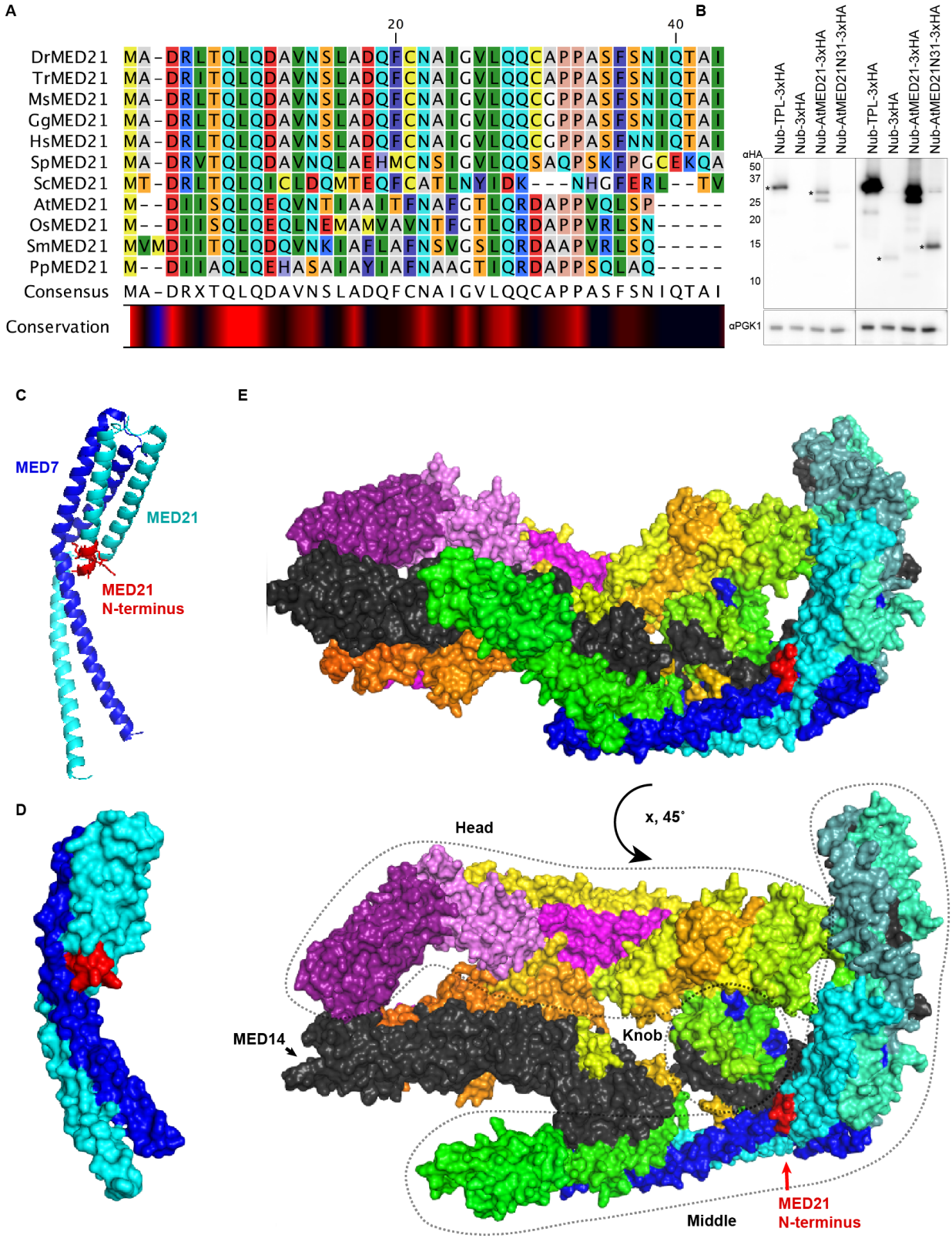

Figure 3 – Figure Supplement 2. Homology and structure of the MED21 subunit of the mediator complex. A. Protein levels of AtMED21 cytoSUS constructs in yeast.

Two different exposure times are shown to demonstrate the lower abundance of the truncation with only the first 31 amino acids of the AtMED21 (N31). Asterisks indicate the size predicted for the indicated protein. **B.** Protein alignment of selected MED21 homologs from various species. Dr - *Drosophila melanogaster*, Tr - *Takifugu rubripes*, Ms - *Mus musculus*, Gg - *Gallus gallus*, Hs - *Homo sapiens*, Sp - *Strongylocentrotus purpuratus*, Sc - *Saccharomyces cerevisiae*, At - *Arabidopsis thaliana*, Os - *Oryza sativa*, Sm - *Selaginella moellendorffii*, Pp - *Physcomitrella patens*. Alignment was performed in CLC sequence viewer 7, using a neighbor joining method. **C-D.** Structure of the MED21 (Cyan) & MED7 (Blue) hetero dimer, adapted from 1YKH, (Baumli et al., 2005). The amino acids in the N-terminus that were solved are highlighted in red up to the 7th amino acid of the yeast MED21. **C.** The cartoon visualization, **D.** Surface visualization. **E.** Core mediator (5N9J, (Nozawa et al., 2017)) with the location of MED21 and MED7 indicated with the same colors from (C-D). In this structure the location of the MED21 N-terminus is again indicated in red, demonstrating its close proximity to the Knob region (dotted circle).

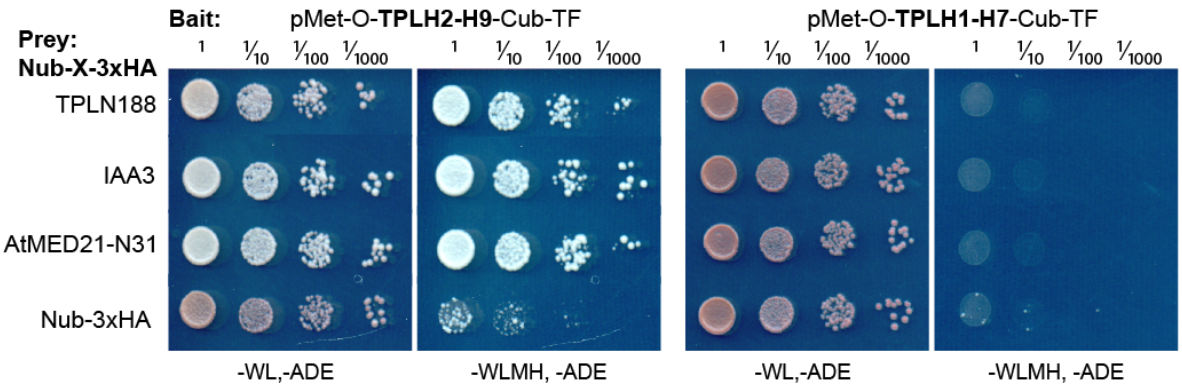

Figure 3 – Figure Supplement 3. TPL interacts with MED21 through an interaction within helices 8-9. Identifying TPL-N terminal domain interactor proteins through cytoplasmic split ubiquitin protein interaction assay. Interaction of bait and prey proteins reconstitute split ubiquitin, release a synthetic transcription factor that allows growth on media lacking Histidine and Adenine. The relative position of the N-terminal portion of ubiquitin (Nub) is indicated for each bait protein. Plates were scanned at 2 days after plating.

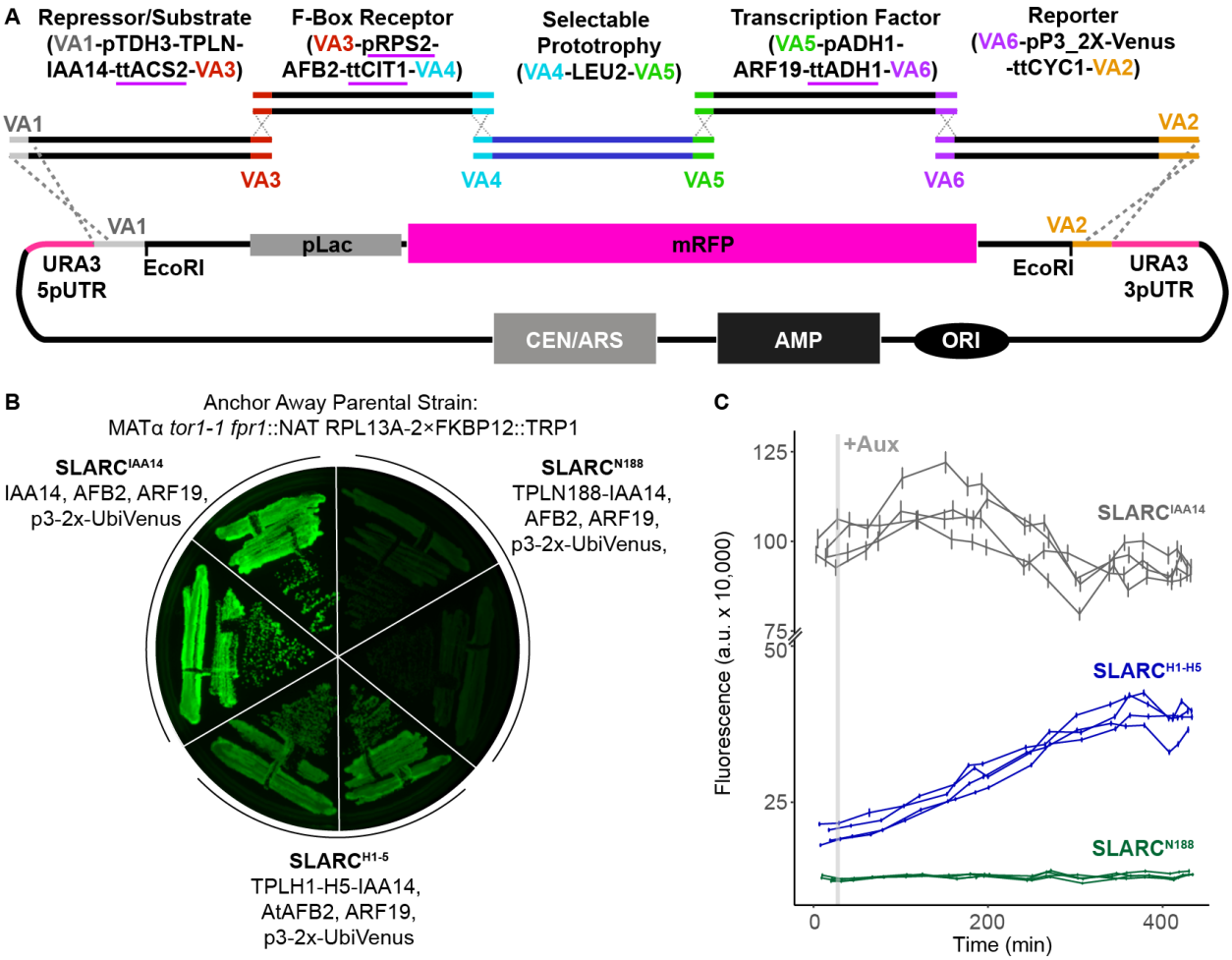

Figure 4 – Figure Supplement 1. Construction and characterization of the Single Locus Auxin Response Circuit (SLARC). A. Design schematic of the approach utilized to create the SLARC through a VEGAS assembly approach. Each individual transcriptional unit (TU) was checked to replace promoters or terminators that utilized identical sequences and replaced with an alternative sequence indicated by a purple underline. These TUs were assembled into level 1 plasmids by Golden Gate reaction. Subsequently, they were amplified by PCR using primers specific for the Vegas Adaptor (VA) sequences specific for their TU cassette. In example, for the first Repressor/Substrate TU the TU was amplified using primers for VA1 and VA3 and purified by a PCR cleanup column (NEB). The acceptor plasmid was cut with EcoRI and both TU and acceptor plasmid was transformed into yeast and recombinant plasmids were selected on synthetic drop out (SDO) plates lacking Leucine. **B.** Primary SLARC transformants were struck out onto fresh SDO -Leu and imaged for Venus expression, demonstrating varying levels of reporter expression that correlate with TPL repressor domains. Plasmid DNA was purified from these strains and sequenced to confirm the proper recombination of TU cassettes. **C.** Time course flow cytometry of SLARC strains

following auxin addition. For all cytometry experiments, the indicated TPL construct is fused to IAA14, because this IAA performs better in haploid yeast strains that IAA3. Every point represents the average fluorescence of 5-10,000 individually measured yeast cells (a.u. - arbitrary units). Auxin (IAA-10μM) was added at the indicated time (gray bar, + Aux). Four independent experiments are shown for each construct.

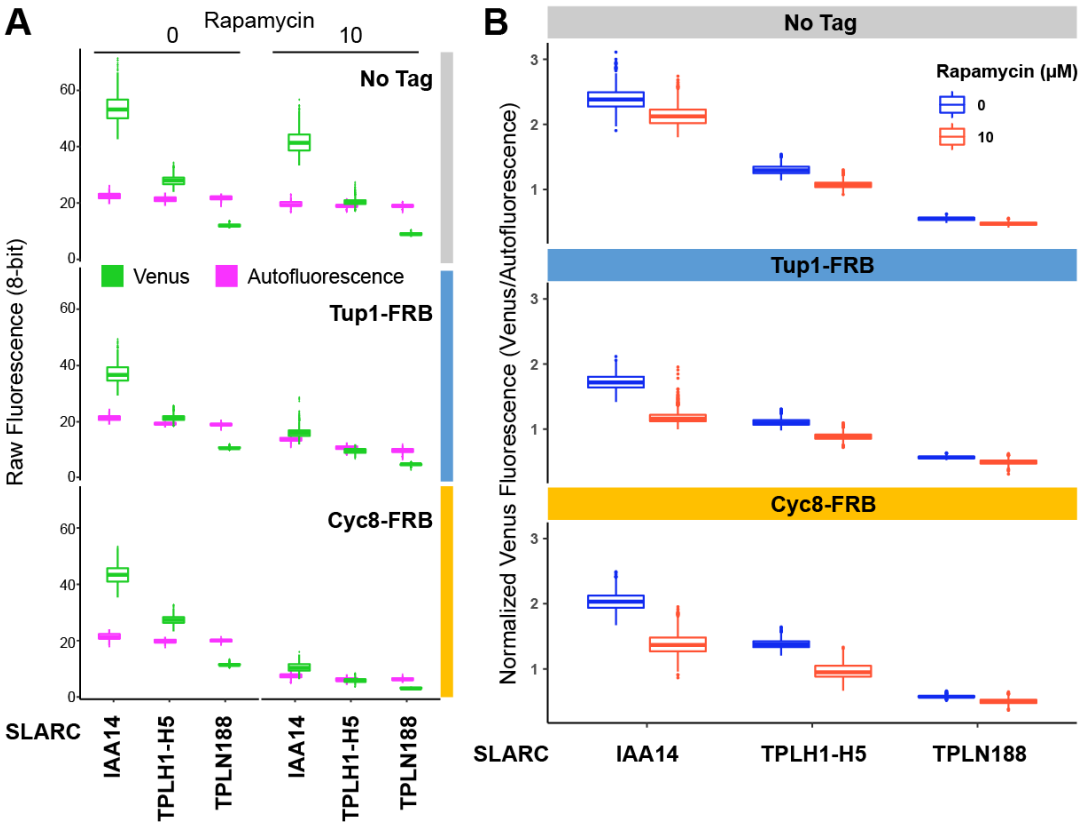

Figure 4 – Figure Supplement 2. The yeast TPL homolog Tup1 and its partner protein do not repress the SLARC. A. Quantified fluorescence from the single locus auxin response circuit (SLARC) introduced into Tup1 and Cyc8 anchor away lines demonstrates no increased fluorescence from the reporter upon depletion of Tup1 or Cyc8 from the nucleus. Data is presented as boxplots, with the Venus reporter in green and the red background (autofluorescence) of the cells plotted in magenta. **B.** Anchor away depletion of Tup1 or Cyc8 results in slower yeast growth. To normalize for this disparity in growth, Venus fluorescence from (**A**) was normalized to red autofluorescence, where each pixel was normalized to the corresponding red autofluorescence collected for that position and plotted as a boxplot. Two individual biological replicates (two separate experiments) were evaluated, and the data was pooled. No increase of reporter signal was detected upon treatment with Rapamycin, indicating that TPL repression does not require either Tup1 or Cyc8 proteins.

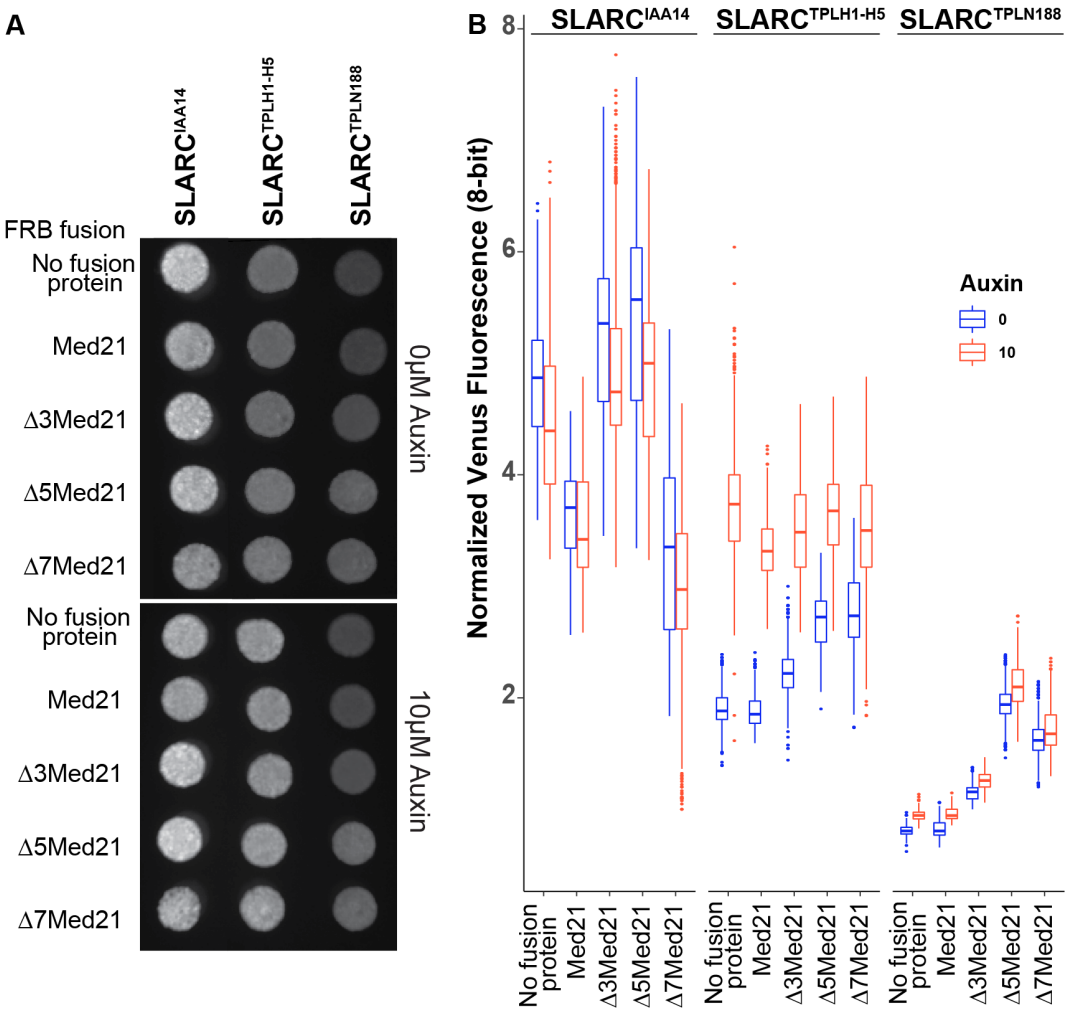

Figure 4 – Figure Supplement 3. MED21 N terminal deletions are viable in *Saccharomyces* and demonstrate altered SLARC transcriptional states. A. A representative grayscale image of fellow fluorescence of spot plates of yeast strains carrying SLARC plasmids in MED21 N-terminal deletions. Each is plated at an OD600 of 0.1 on SDO with or without auxin (10μM IAA). **B.** Venus fluorescence from (**A**) was normalized to red background (autofluorescence), where each pixel was normalized to the corresponding red autofluorescence collected for that position and plotted as a boxplot. Two individual biological replicates (two separate experiments) were evaluated, and the data was pooled and is presented as boxplots.

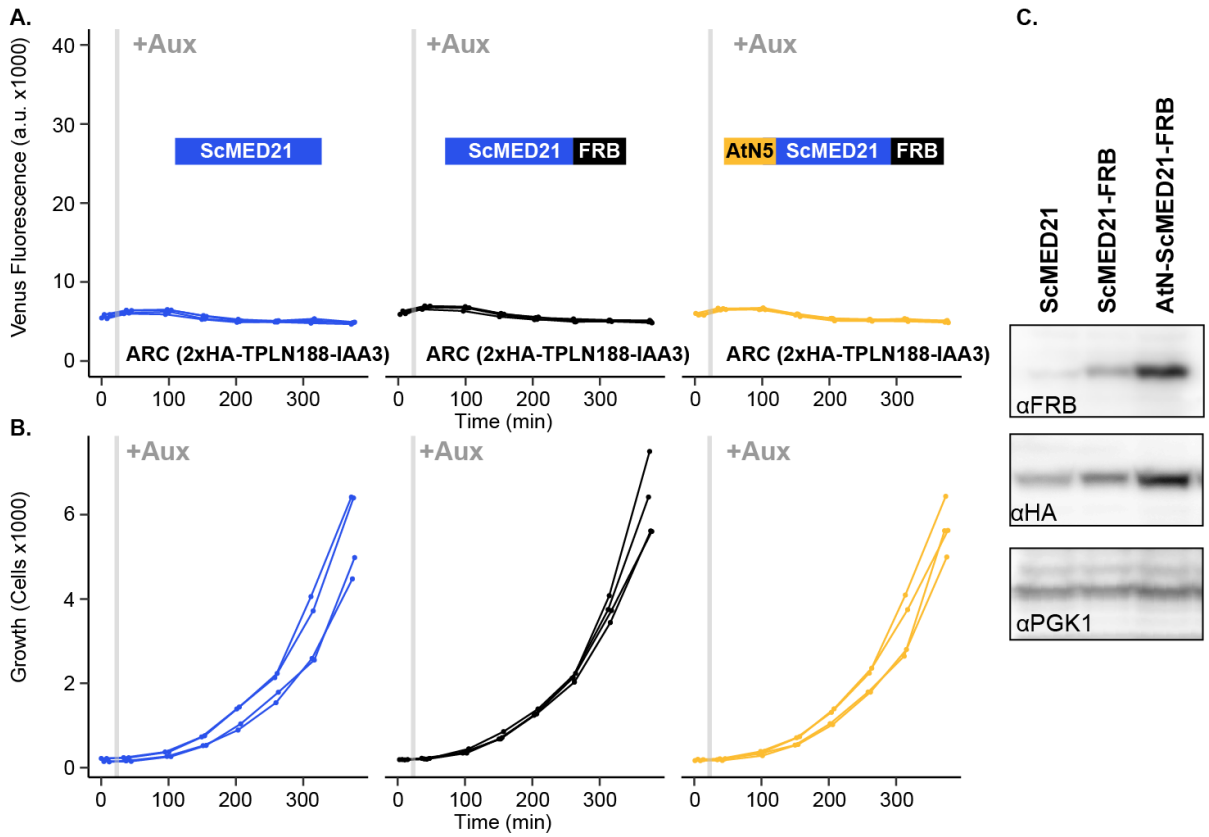

Figure 4 – Figure Supplement 4. A. Conversion of the first five amino acids of ScMED21 to the corresponding sequence from AtMED21 results in an identical repression profile. Time course flow cytometry of SLARC strains following auxin addition. For all cytometry experiments, the indicated TPL construct is fused to IAA14, because this IAA performs better in haploid yeast strains that IAA3. Every point represents the average fluorescence of 5-10,000 individually measured yeast cells (a.u. - arbitrary units). Auxin (IAA-10μM) was added at the indicated time (gray bar, + Aux). Two independent experiments are shown for each construct. **B.** Cell growth of the strains in (**A**) indicate the swap of the N-terminal region had no effect on yeast growth or viability. Data presented is events per microliter over the time-course of the cytometry experiments. **C.** Protein expression analysis by western blotting of strains used in A & B. In this ARC, TPLN188-IAA3 is N-terminally fused to 2xHA. Total protein loading levels were tested by blotting against the housekeeping gene PGK1 (bottom panel).

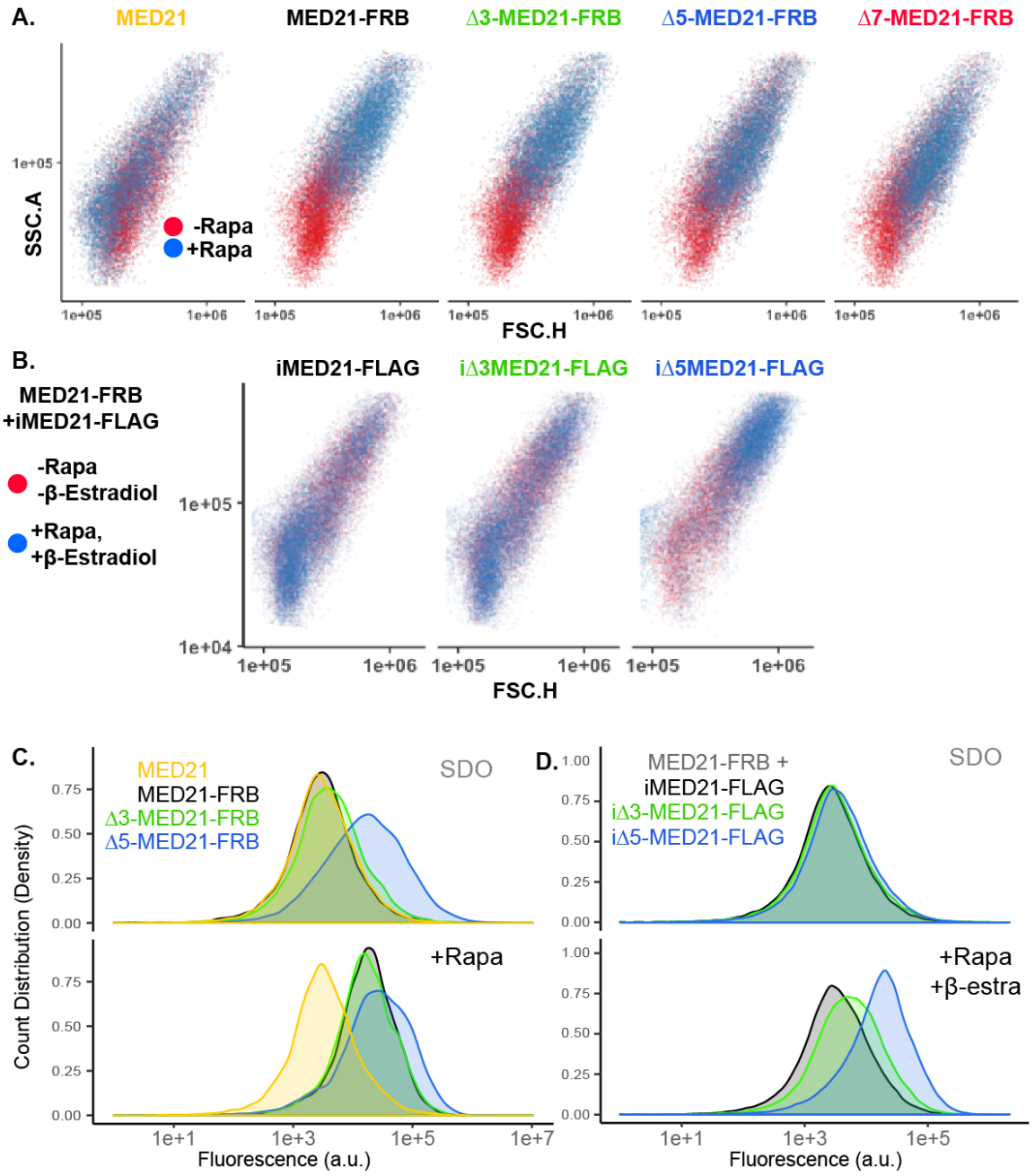

Figure 4 – Figure Supplement 5. Inducible MED21 rescues rapamycin induced yeast growth defects. A. Depletion of nuclear ScMed21 by Rapamycin increased cell size even in short time-courses, consistent with its essential role in many core pathways. Scatterplots of side scatter area by forward scatter height (SSC.A x FSC.H) indicate large scale increases in cell size in populations of yeast with (blue) or without (red) Rapamycin treatment. **B.** Inducible MED21 (iMed21) wild type and variants cell size were examined before (red) and after (blue) treatment with Rapamycin and β-estradiol to simultaneously deplete the wild-type ScMed21-FRB fusion, and induce the transcription of the MED21 variant. Scatterplots of side scatter area by forward scatter

height (SSC.A x FSC.H) demonstrate a less disrupted cell size compared to Anchor Away strains in (**A**). **C-D.** Histograms of Venus fluorescence in inducible MED21 (iMed21) strains demonstrate that populations were evenly distributed around a single mean, suggesting we were observing the immediate effects of the MED21 deletions. The histograms were built using ggplots Density function to create a visualization of count distribution. These samples were tested at 300 minutes (as in Figure 4D), and plotted to visualize cells at the equivalent stage of growth, MED21 depletion, and induction. **C.** Effect of anchor away of ScMed21-FRB variants alone and **D.** Depletion of ScMed21-FRB after induction (β-estradiol added 4 hours before Rapamycin treatment) of iMed21.

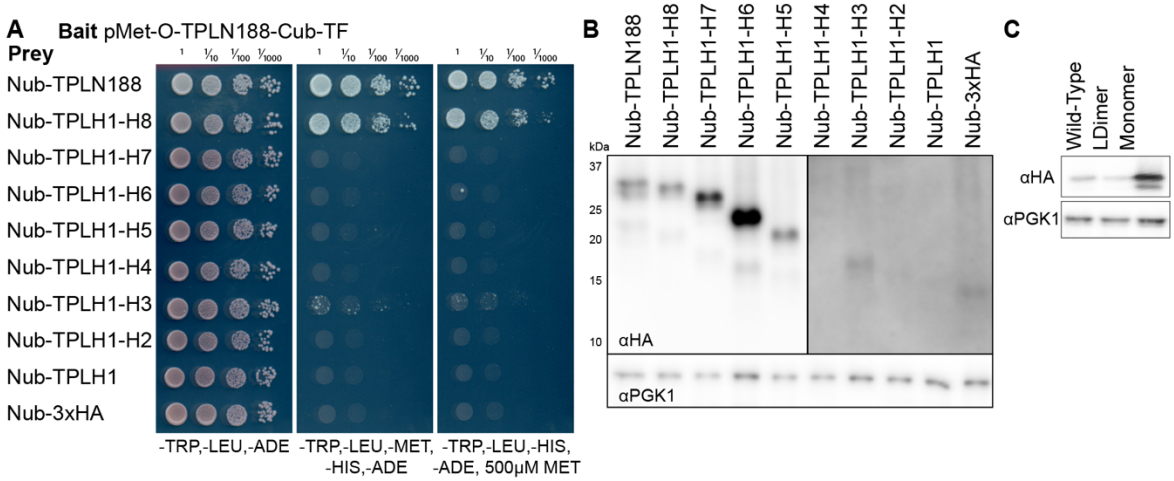

Figure 5 – Figure Supplement 1. A. Cytoplasmic split ubiquitin interaction (cytoSUS) assay on serial deletions of TPL. Interaction of bait and prey proteins reconstitute split ubiquitin, release a synthetic transcription factor that allows growth on media lacking Histidine and Adenine. The expression level of the bait protein can be repressed through increased Methionine in the media. **B**. Protein levels of Nub-TPL fusions were tested by PAGE and western blotting for the c-terminal 3xHA epitope tag included in all constructs. Deletions longer than H1-4 are detectable at higher levels (left panel), whereas shorter isoforms required longer exposure times to detect (right panel). Total protein loading levels were tested by the housekeeping gene PGK1 (bottom panel). **C.** Protein expression analysis by western blotting of tetramerization mutants expressed in yeast for cytoSUS interaction assay in Figure 5I. Prey constructs are C-terminally fused to 2xHA. Total protein loading levels were tested by blotting against the housekeeping gene PGK1 (bottom panel).

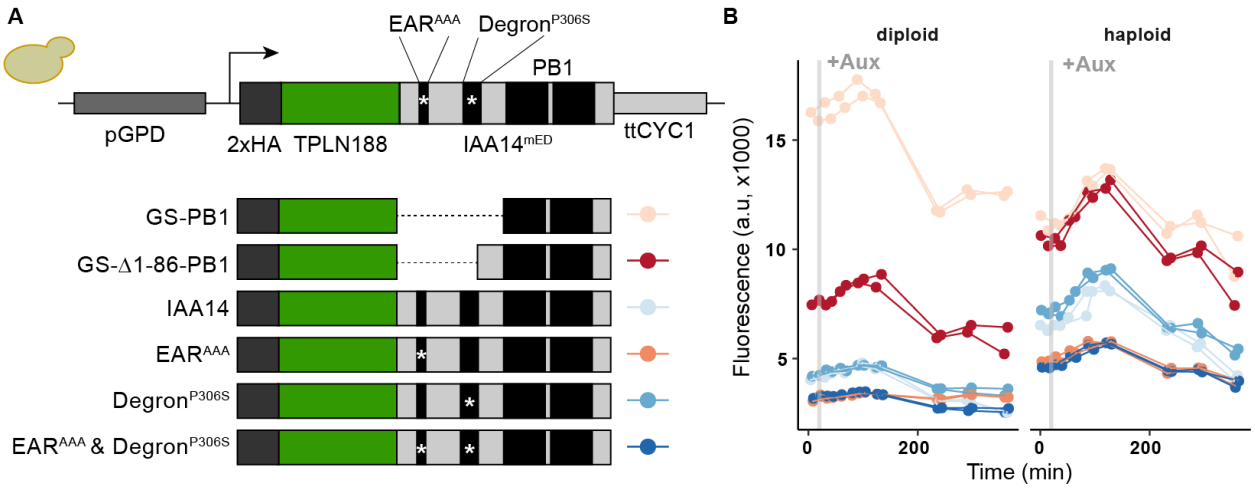

Figure 6 – Figure Supplement 1. Engineering and prototyping a variant of TPLN-IAA14^{mED} which carries mutations in the EAR domain (EAR^{AAA}) and in the degron (P306S) in yeast. A. Cartoon schematic of the mutations tested during prototyping of the TPLN188-IAA14mED construct. In each case the identical glycine-serine linker (GS) was used as the flexible linker between the 2xHA-TPLN188 protein and the portion of IAA14 retained in the construct. **B.** Time course flow cytometry of TPLN-IAA14^{mED} strains following auxin addition. Strains containing the TPLN-IAA14^{mED} was tested in both haploid and diploid strains and demonstrated similar repression profiles. Every point represents the average fluorescence of 5-10,000 individually measured yeast cells (a.u. - arbitrary units). Auxin (IAA-10μM) was added at the indicated time (gray bar, + Aux). Two independent experiments are shown for each construct.

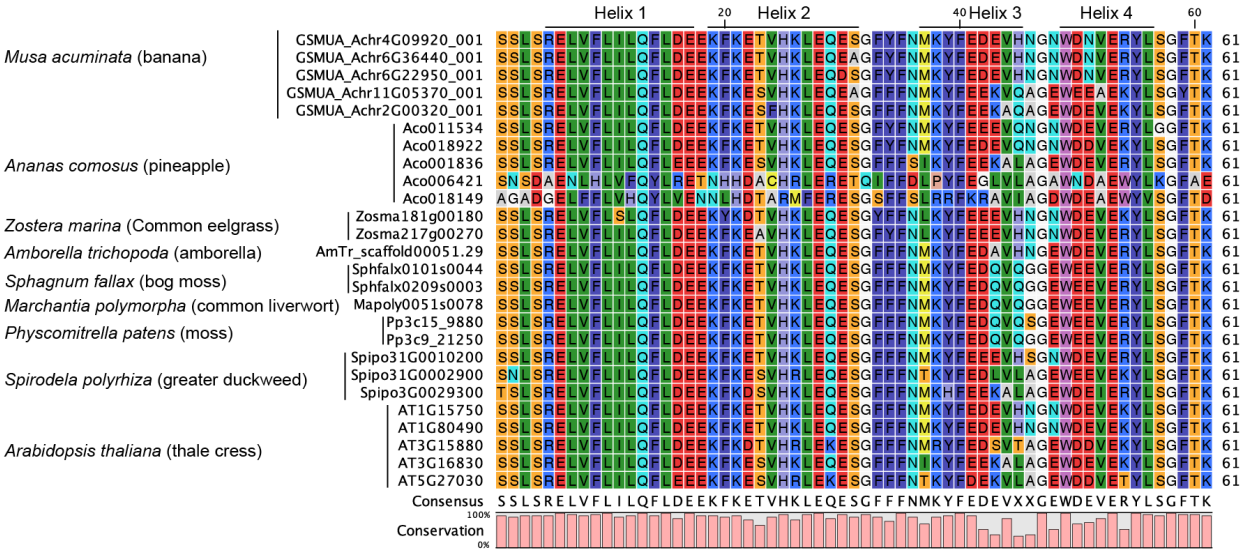

Figure 6 – Figure supplement 2. Alignment of TPL homologs demonstrates high levels of conservation over the LisH domain (Helix 1 – Helix 2) in the land plant lineage. Amino acid sequences from Phytozome (https://phytozome.jgi.doe.gov/) were identified by homology to TPL and TPR sequences from *Arabidopsis thaliana*. Sequences were aligned using CLC sequence viewer and amino acids are shaded according to the RASMOL color scheme. High levels of conservation can be observed within the LisH domain. Sequences are grouped by species, and the species name is provided on the left.

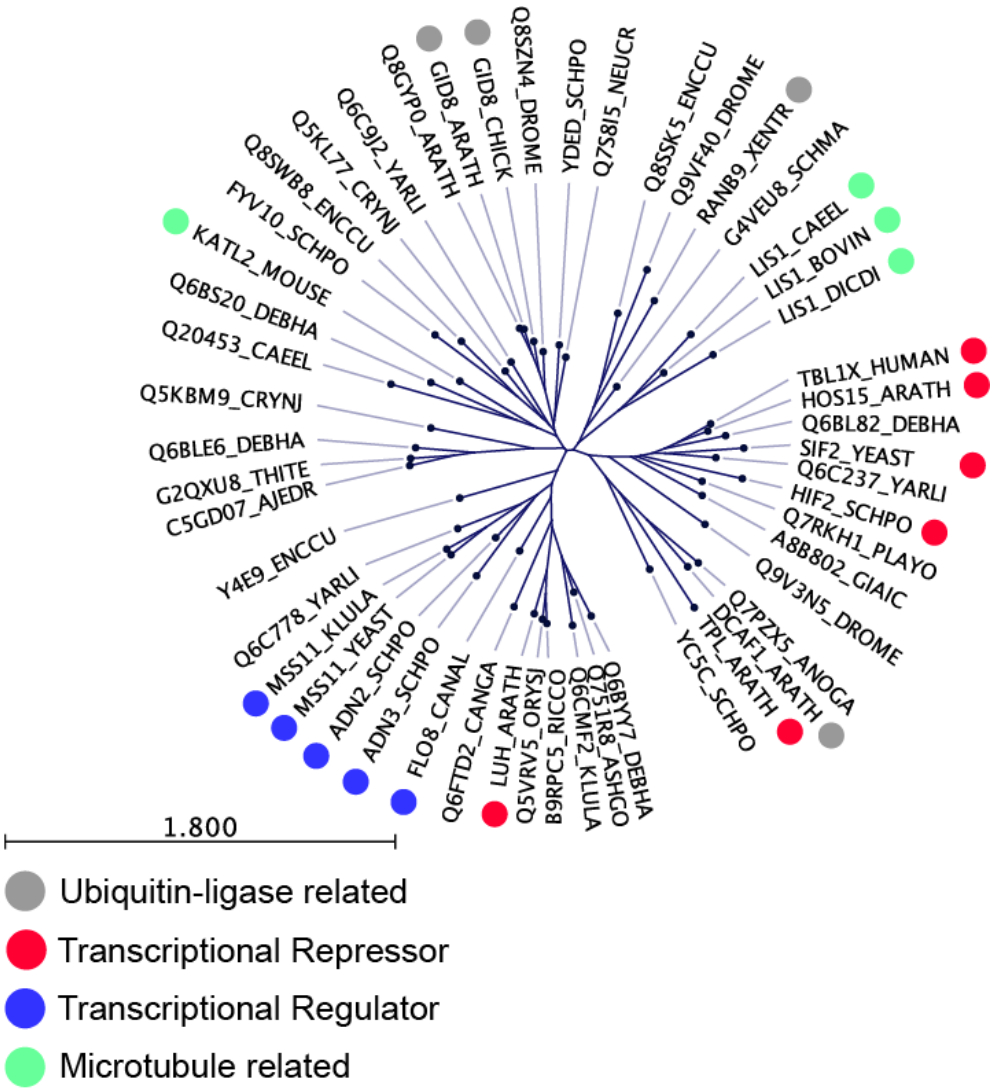

Figure 6 – Figure Supplement 3. Phylogenetic tree of seed LisH domains in the PFAM08513 Seed alignment identify a subclade of proteins with defined repressor functions. The TPL LisH domain was added to an alignment of seed sequences for PFAM08513 containing 50 seed sequences (the curated alignment from which the HMM for the family is built). These were aligned using CLC Sequence Viewer 7, a tree was constructed using a Neighbor Joining method, and bootstrap analysis performed with 10,000 replicates. Colored circles were added to proteins where functional analysis has yielded functional information about gene function.

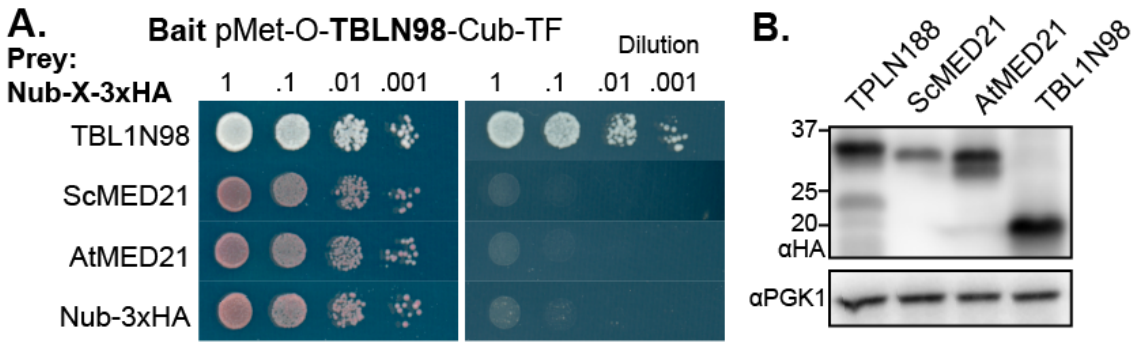

Figure 6 – Figure Supplement 4. A. Identifying TBL1 N-terminal domain interactor proteins through cytoplasmic split ubiquitin protein interaction assay. TBL1N98 interacts with itself in yeast, but not with AtMED21 nor ScMED21. **B.** Protein abundance of TBL1N98 was tested by SDS-PAGE & western blot. Prey constructs are C-terminally fused to 2xHA. Total protein loading levels were tested by blotting against the housekeeping gene PGK1 (bottom panel).